

## Resum

El CERN és el Consell Europeu de la Investigació Nuclear. Actualment s'està construint el més gran i potent accelerador de partícules del món. L'anomenat Large Hadron Collider (LHC) situant-se a la frontera franco-suïssa, ocupant una superfície de 27Km i a una profunditat de 100m sota terra. Al llarg d'aquesta circumferència es localitzaran 4 grans detectors de partícules, ATLAS, CMS, LHC-b i ALICE.

Als dos costats del CMS s'ubica l'experiment TOTEM que té com objectiu mesurar l'angle de desviació de les partícules que provenen de la col·lisió al CMS i és la fita del present projecte.

Per tal de poder dur a terme aquest projecte cal construir 3 estacions a cada costat del CMS. En aquestes estacions es localitzaran els Roman Pots que tenen la finalitat de subjectar els aparells que contindran els detectors. Tot el sistema estarà connectat per un sistema de refrigeració que evacuarà la calor que prové del flux de partícules una vegada aquest hagi passat a través dels detectors.

El detector estarà subjectat per l'anomenat "Thermal Model". Aquest projecte consisteix en la creació del prototip "Thermal Model", l'estudi d'un sistema termodinàmic que ajudarà a simular les conseqüències que poden afectar sobre el sistema una vegada el flux de partícules l'hagi travessat.

S'haurà de fer un estudi termodinàmic i mecànic detallat i treure'n conclusions. Depenent dels resultats s'haurà de modificar el model per a que estigui perfectament adaptat per l'experiment que es durà a terme a l'any 2007.

La planificació d'aquest projecte va començar en el disseny del prototip, creant un conjunt de 10 cartes que cadascuna d'elles subjectarà un detector. Aquestes cartes estan comprimides per uns marcs de coure. De l'extrem superior d'aquestes peces en surt el sistema de refrigeració que consta de 4 heat pipes i aquestes es connecten a una gran heat pipe que desenvoca al pulse tube.

Per arribar a la conclusió de quin tipus de heat pipe s'ha d'utilitzar, quin gas és el més adequat per extreure i conduir la calor, quines són les millors dimensions i amb quin angle es podrien inclinar les heat pipes, s'han hagut de fer una serie d'experiments.

L'estudi termodinàmic ha consistit en situar raonadament 40 sensors de temperatura sobre el prototip. També s'han posicionat 11 strain gauges per mesurar la deformació de la peça per causa de la calor. Amb l'ajuda dels programes LabVIEW i ANSYS s'han pogut treure unes acurades conclusions.

Actualment s'està pensant amb com modificar el prototip "Thermal Model".





# Contents

<b>RESUM</b>	<b>1</b>
<b>CONTENTS</b>	<b>3</b>
<b>1 GLOSSARY</b>	<b>6</b>
<b>2 INTRODUCTION</b>	<b>8</b>
2.1 Motivation of the project.....	8
2.2 Aim of the project.....	8
2.3 Scope of the project.....	9
<b>3 INTRODUCTION TO CERN</b>	<b>10</b>
<b>4 TOTEM AT LHC POINT 5</b>	<b>17</b>
4.1 Roman Pot .....	18
4.1.1 Roman Pot Technique.....	18
4.1.2 The Pot .....	18
4.2 Roman Pot Station.....	20
4.3 Cooling Proposed .....	22
<b>5 COOLING SYSTEM</b>	<b>24</b>
5.1 Heat Pipes .....	24
5.1.1 Theory .....	25
5.1.2 Performance limits .....	26
5.2 Heat Pipes operation prediction .....	31
5.2.1 Gravity Aided:.....	31
5.2.2 Horizontal: .....	31
5.2.3 Against Gravity:.....	31
5.3 Types of the heat pipes used .....	33
5.4 Working fluid .....	35
5.5 Application to Prototype Cooling System .....	36
5.6 Loop Heat Pipes .....	37
5.6.1 Technical conclusion .....	37
5.7 Pulse Tube .....	38
5.8 Radiation Environment .....	42
5.9 Conclusions .....	43



<b>6</b>	<b>PROTOTYPE COOLING SYSTEM AND ROMAN POT THERMAL MODEL</b>	<b>44</b>
6.1	Planning.....	46
6.2	Designing the Model.....	48
6.3	Temperature sensors location of the Thermal Model.....	49
6.4	Mechanical study of the Thermal Model.....	53
6.5	Assembly of the instruments on the Model.....	60
6.6	Preparing of a Data Acquisition in LabView .....	62
<b>7</b>	<b>TEST OF THE MODEL AND COOLING SYSTEM</b>	<b>64</b>
7.1	Data Analysis .....	64
7.1.1	Thermal Test Station.....	64
7.1.2	Test Set-up for Roman Pot Thermal Model .....	65
7.1.2.1	Temperatures on the copper frames-side.....	65
7.1.2.2	Temperatures on the copper frames-surfaces .....	68
7.1.2.3	Temperatures on the PCB cards .....	69
7.1.2.4	Temperatures on heat transfer system .....	74
7.2	Conclusion.....	75
<b>8</b>	<b>FUTURE DEVELOPMENTS</b>	<b>77</b>
<b>9</b>	<b>CONCLUSIONS</b>	<b>78</b>
<b>10</b>	<b>ACKNOWLEDGEMENTS</b>	<b>81</b>
<b>11</b>	<b>REFERENCES</b>	<b>83</b>





# 1 Glossary

Explanation of the terms used in this document:

**CERN:** CERN is the European Organization for Nuclear research. It is the world's largest particle physics laboratory.

**LCH:** the term LHC stands for **Large Hadron Collider**, the new particle accelerator under construction at CERN. Full details are given in section 3.2.

**IP (Interaction Points, Experimental Points):** Points of the LHC where the two particles bunch travelling in opposite senses collide against each other.

**TOTEM:** Total Cross Section, Elastic Scattering and Diffraction Dissociation at the LHC.

**RP: Roman Pot** is an experimental technique for the detection of forward protons from elastic or diffractive scattering.

**LabVIEW (Laboratory Virtual Instrument Engineering Workbench).** LabVIEW is a graphical programming language that uses icons instead of lines of text to create programs.

**VI (Virtual Instrument):** Program in LabVIEW that models the appearance and function of a physical instrument.

**BEAM:** the beam referred to in this project is *not* the LHC beam, but rather the flux of these scattered particles which TOTEM seeks to measure.

**FEM (Finite Element Model):** It is when you break the model into thousands of nodes and calculated the deformation at each node (point).





## 2 Introduction

### 2.1 Motivation of the project

CERN is the European Organization for Nuclear research. It is the world's largest particle physics laboratory. CERN currently employs engineers, physicists and many other people to conduct research using modern technology. It is an international community and this environment gives the possibility to improve language skills. For all of these main reasons I have always been full of enthusiasm and motivation with the idea of one day working at CERN as a member of a group developing a project.

When CERN proposed that I carry out a part of a thermodynamics project, I accepted because it had crucial importance in my personal and engineering skills development.

The origin of this project arises from the need to extract heat created by electronic components associated with a particle detector in the TOTEM experiment. To achieve this goal a heat exchanger must be created. Before creating the final version of the exchanger to be used in the TOTEM experiment, prototypes must be built in order to study and evaluate the ability to extract the heat and keep the temperature constant. The results of these studies can then be used to solve any existing problems, to remove possible flaws, and to propose changes in the design of the final system to be used in the TOTEM experiment.

I was in charge of planning a thermodynamic system to control the temperatures on one of the prototypes denominated during this work as the Thermal Model.

### 2.2 Aim of the project

The thermodynamic objective of the project entitled, "Thermal Model", is to extract the heat released by the detector when the beam passes through it and to establish an average temperature suitable for safe operation of the various detector components. To accomplish this objective, a system of four Heat Pipes will be used. They will transport the heat from the model towards another large Heat Pipe. This final Heat Pipe will lead the heat towards a Pulse Tube.

Basically the aim of the project is to detail the main activities to be followed in order to plan, design, study the thermodynamics, prepare a data acquisition system, and successfully obtain the expected results.



## 2.3 Scope of the project

The scope of the project involves determining which are the best types of heat pipes that can be used, which kind of gas is adapted to extract and to conduct the heat, which are the best dimensions and at which angle the heat pipes can be inclined. A series of experiments are foreseen in order to answer these questions.

The thermodynamic study has consisted of locating 40 temperature sensors on the prototype. Also, eleven strain gauges have been positioned to measure the deformation of the piece caused by the heat. With the aid of programs such as LabVIEW and ANSYS, specific conclusions can be made.

The deadline for the TOTEM project completion is next October. Every thing has to be ready at that time for installation at the Point 5, where the TOTEM experiment will be located.



### 3 Introduction to Cern

CERN is a European Organization for Nuclear Research, founded in 1954. It is a laboratory where scientists unite to study the building blocks of matter and the forces that hold them together and to reach a better understanding of the behavior of the universe. *A grosso modo*, the idea to combine the national science laboratories of Europe into one big science organization was born in 1949 and was first proposed by the French physicist and noble-prize winner Louis de Broglie.

CERN is located on both sides of the France-Swiss border in the north of Geneva. (Figure. 3.1). Nowadays CERN is composed of 20 member States: Austria, Belgium, Bulgaria, Czech Republic, Denmark, Finland, France, Germany, Greece, Hungary, Italy, Netherlands, Norway, Poland, Portugal, Slovak Republic, Spain, Sweden, Switzerland and the United Kingdom (Figure. 3.2) [1].

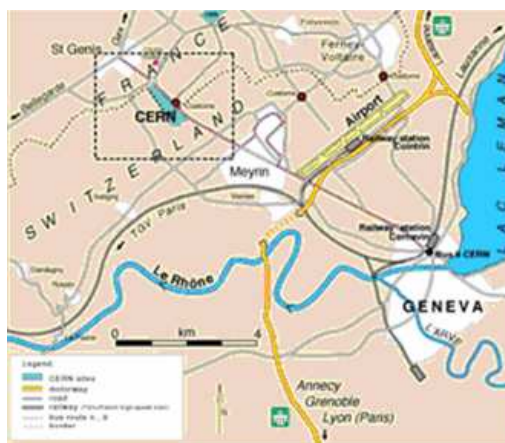


Fig. 3.1 Cern's location



Fig. 3.2 the twenty Member States of CERN



CERN builds and operates the particle accelerators needed for particle physics research in a unique centre which allows physicists around Europe to collaborate more fruitfully than if each country maintained an independent program.

In the first three years after its opening, CERN worked on the construction of its first particle accelerator. In 1957, the proton Synchro-Cyclotron (SC) was switched on and after a short time, recorded the first results of pions decaying into an electron and a neutrino, as predicted by the weak interaction theory. The machine worked at a total collision power of a 600MeV. This power was multiplied by almost 50 when only two years later, CERN's first major machine, the Proton Synchrotron (PS), came into operation. With its 24GeV power with which the protons collide, it was the biggest accelerator in the world.

In 1981, the CERN council approved the construction of a 27km circumference Large Electron-Positron collider (LEP) ring, the largest scientific instrument ever created, for an initial operating energy of 50GeV per beam. This new instrument led to very accurate measurements of the Z-boson decay and confirmed the Standard Model of particle physics.

At present, CERN is building the Large Hadron Collider (LHC) in the old tunnel of the LEP experiment (FigureX). Two large detector experiments, ATLAS (*A Toroidal LHC Aparatus*) and CMS (*Compact Muon Solenoid*), will look for the Higgs boson, a particle predicted by the latest theories of modern physics. After the estimated start of these detector experiments, the LHC will collide protons with an energy of 14TeV. Besides the acceleration of protons, the LHC will accelerate lead nuclides up to a total collision power of 1150TeV which is almost equal to the power density in the universe short after the Big Bang. Together with ATLAS and CMS, two other experiments will be fed by the LHC: a dedicated heavy ion detector, ALICE, which will be built to exploit the unique physics potential of nucleus-nucleus interactions at LHC energies, and LHC-B, which will carry out precision measurements of CP-violation and rare decays of B mesons (*Figure 3.3*). Because of the huge amount of events produced during operation, 800 million collisions per second, the detectors and the computer facilities have to handle as much information as the whole European telecommunication networks combined.

Not only high energy physics are practiced at CERN. The desire to discover new physical laws led to many new inventions in the fields of informatics and engineering. Tim Berners-Lee proposed in 1990 a distributed information system, based on 'hypertext'. By hiding network addresses behind highlighted items on the screen, information can be linked between several computers. The chosen name for this new invention was the "World-Wide Web".



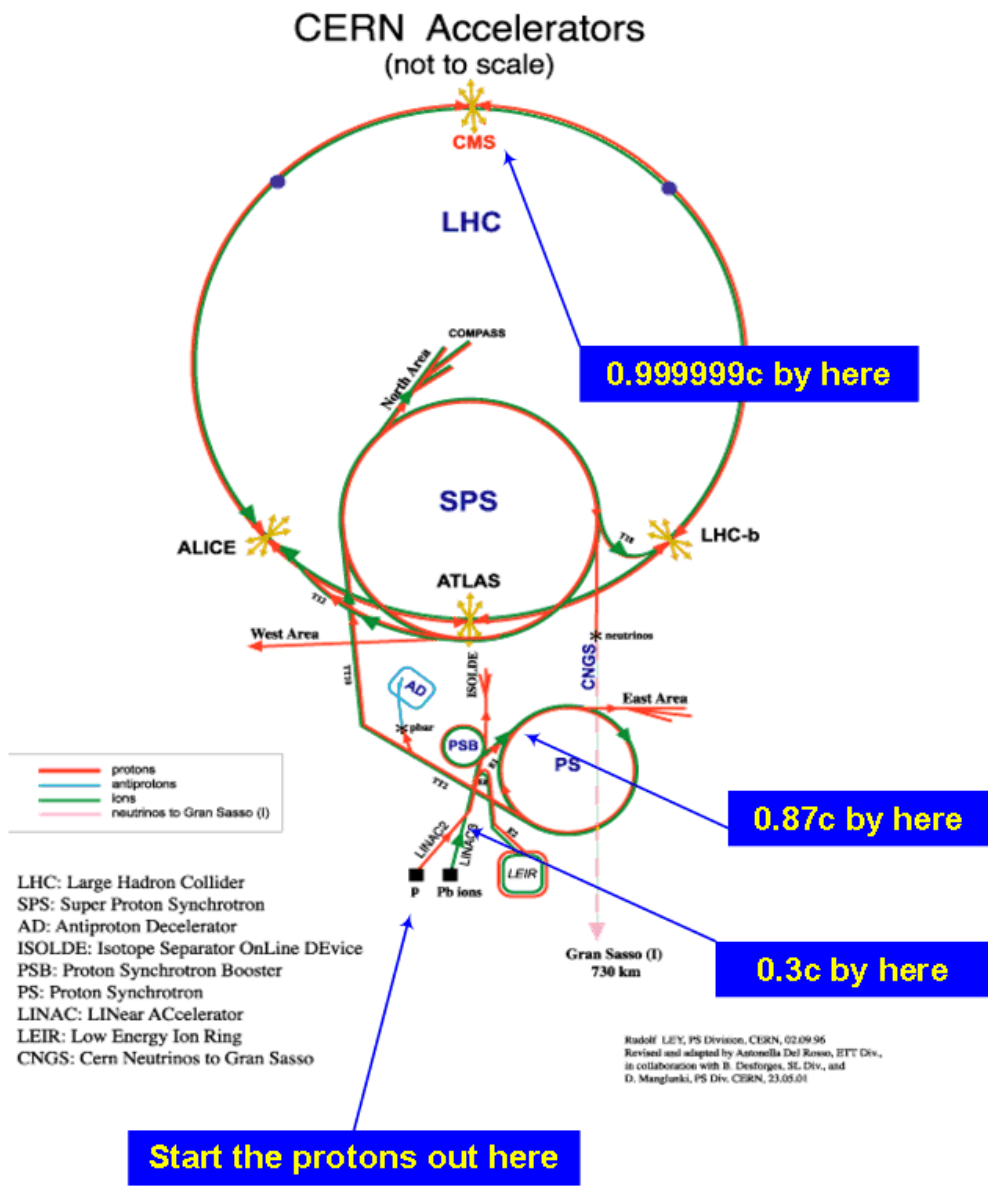


Fig. 3.3 The CERN network of interlinked accelerators and colliders.



### The Large Hadron Collider (LHC)

The Large Hadron Collider [2] will collide two counter-rotating proton beams at a centre-of-mass energy of 14TeV. This energy is seven times higher than the beam energy of any other proton accelerator to date. In order to achieve an unprecedented luminosity of  $1034 \text{ cm}^{-2}\text{s}^{-2}$ , it must operate with more than 2800 bunches per beam and a very high intensity. The machine can also be filled by lead ions up to 5.5TeV/nucleon and therefore allow heavy-ion experiments at energies about thirty times higher than at the Relativistic Heavy Ion Collider (RHIC) at the Brookhaven National Laboratory in New York. Some of the parameters of the new accelerator are listed in the (Table 3.1):

Constants of the LHC	Value
Energy	<b>7 TeV</b>
Injection Energy	<b>0.45 TeV</b>
Dipole Field	<b>8.36 Tesla</b>
Number of dipole magnets	<b>1232</b>
Number of quadruple magnets	<b>430</b>
Number of corrector magnets	<b>8000</b>
Luminosity	<b><math>1034 \text{ cm}^{-2}\text{s}^{-1}</math></b>
Coil aperture in arcs	<b>56 mm</b>
Distance between apertures	<b>194 mm</b>
Particles per bunch	<b>1011</b>
Number of Bunches	<b>2835</b>

Table 3.1 Summary of the LHC parameters [3]



The primary task of the LHC is to make an initial exploration of the 1TeV range. The major LHC detectors, ATLAS (*A Toroidal LHC AparatuS*) and CMS (*Compact Muon Solenoid*) should be able to accomplish this for any Higgs mass in the expected range. To get into the 1TeV scale the needed beam energy is 7TeV.

## LHC Layout

The LHC has an eight-fold symmetry with eight arc sections and eight long straight sections. Two counter-rotating proton beams will circulate in separate beam pipes installed in the same magnet (*twin-aperture*). The beams will cross over at the four experiments resulting in an identical path length for each beam (*Figure 3.4*).

Each arc consists of 23 identical cells, giving the total length of 2465m. Cells are formed by six 15m dipole magnets and two quadrupole magnets (these dipoles and quadrupoles are called lattice or main magnets). Dipole magnets are used to deflect the beam in a circular trajectory whereas quadrupole magnets act as lenses to focus the beam. The lattice quadrupole magnets and the corrector magnets of a particular half-cell form a so called short straight section (SSS) and are housed in a common cold mass and cryostat.

At the beginning and the end of the straight sections a dispersion suppressor cell, consisting of four quadrupole interleaved with four strings of two dipoles each, is in charge of correcting the orbital deviation due to the drift in the energy of the particles. The four long straight sections where the experiments are located are formed by the dispersion suppressors and the insertion magnets. These insertion magnets guide the separated beams to a common pipe where they are focused by the so called inner triplet magnets in order to get even tighter beams before the collisions take place inside the detectors.

Other insertions are to be used by systems for the machine operation: beam dump, beam cleaning (collimation), RF-cavities (accelerator units) and injection from pre-accelerators.

The injector complex includes many accelerators at CERN: linacs, booster, LEAR as an ion accumulator, PS and the SPS. The beams will be injected into the LHC from the SPS at an energy of 450GeV and accelerated to 7TeV in about 30 min. They can they be used to collide for many hours.



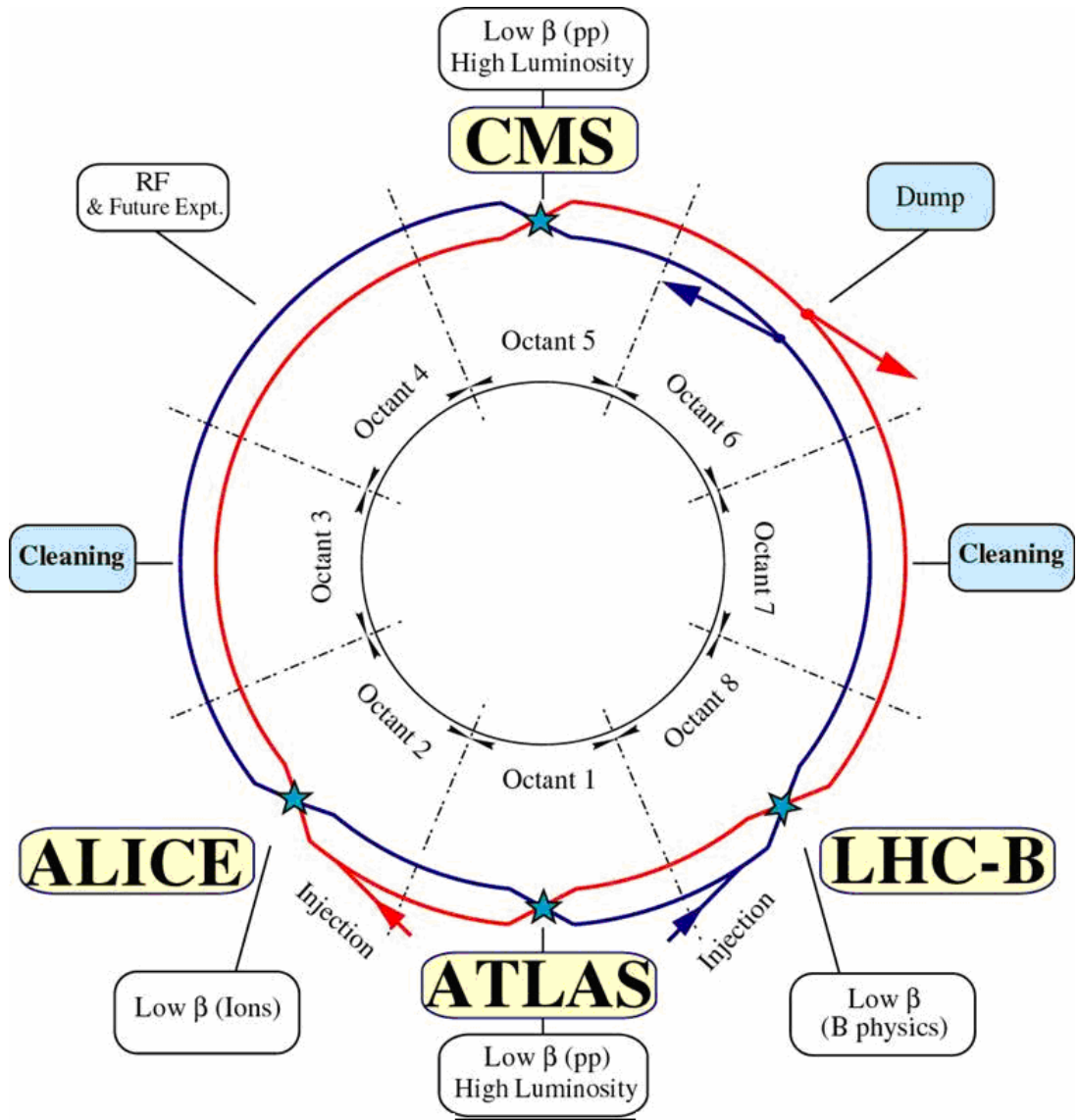


Fig. 3.4 LHC layout



## LHC and TOTEM

The LHC is CERN's major project. The commissioning of this 27km circumference superconducting proton-proton collider with its four large scale experiments, ATLAS, CMS, LHC-B and ALICE is expected for 2007. The fifth experiment, TOTEM, is particular in its composition with inelastic detectors in the forward region of CMS and with numerous small sub-detectors extending over large distances along the LHC tunnel. (Figure 3.5) gives a principle lay-out of the LHC with its five experiments. The distant sub-detectors called "roman pot detectors" require cooling. Different cooling methods have been studied and their feasibility investigated for the LHC collider environment. The adopted solution is described in the following report.

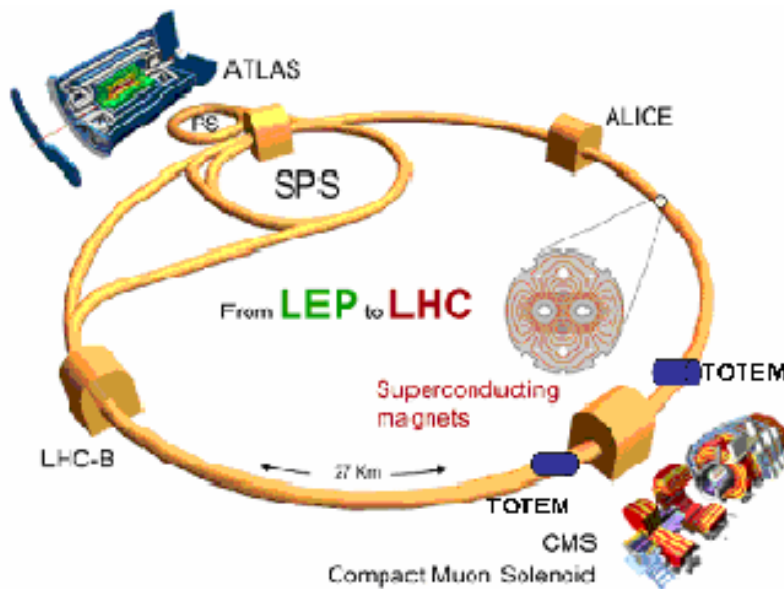


Fig. 3.5 TOTEM locations at LHC



## 4 TOTEM at LHC point 5

TOTEM is the main objective on this project.

TOTEM is an experiment at the CERN LHC collider to measure the total p-p cross section and elastic scattering of protons. The detection of the elastically scattered particles at very small angles with respect to the beams edgeless silicon detectors will be contained in 36 small vacuum vessels called “roman pots” to be installed inside the LHC beam vacuum pipe. The final –not yet fixed- operating temperature is expected to be around 220K. The preferred cooling method applies a combination of cryogenic heat pipes and pulse tube refrigerators [4]

TOTEM is located close to the beam pipe on either side of CMS, exactly at the LHC point 5.

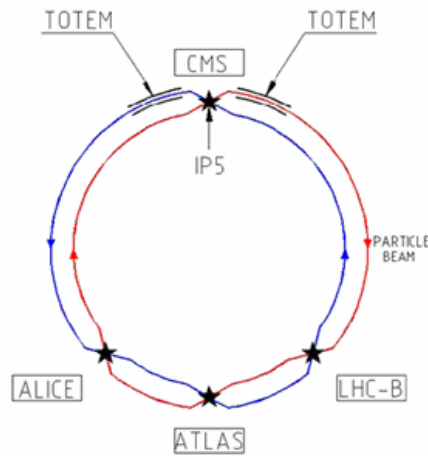


Fig. 4.1 TOTEM at LHC point 5

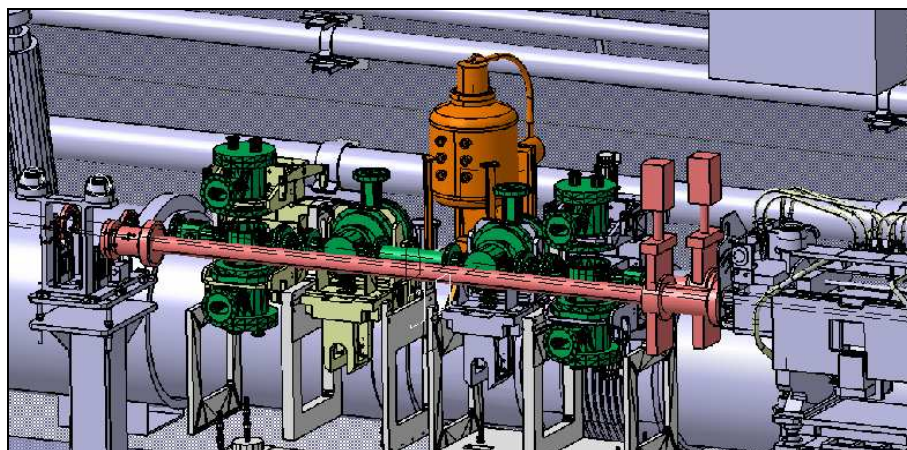


Fig. 4.2 Layout of the LHC-TOTEM



## 4.1 Roman Pot

### 4.1.1 Roman Pot Technique.

The Roman Pot is an experimental technique introduced at the ISR2 for the detection of forward protons from elastic or diffractive scattering and has been successfully installed in other machines like the SPS3, TEVATRON4, RHIC5 and DESY6 [5].

Detectors are placed inside a secondary vacuum vessel, called *pot*, and moved into the primary vacuum of the machine through vacuum bellows. In this way the detectors are physically separated from the primary vacuum which is preserved against an uncontrolled out gassing of the detector's materials. In order to minimize the distance of the detectors from the beam, the wall thickness of the pot is locally reduced to a thin window foil which has also the benefit of minimizing the effects of unwanted secondary interactions.

Together with the choice of the detector technology and their integration, crucial aspects of this technique are the mechanical stability and robustness of the thin foil. The change of the beam impedance and the pick-up noise on the detector due to the bunched structure of the beam must be minimized. The compatibility of the Roman Pot operation with the machine protection system is crucial at the LHC, since for physics performance, detectors have to be placed very close to high intensity beams. The challenging constraints of the LHC, such as the narrow high-intensity beam with energy of 7TeV, the Ultra High Vacuum and the high radiation fluxes, required the development of new Roman Pots. The challenges lay in the flatness of the thin window at the bottom of the pot, in the driving mechanism, in the accuracy of the movement and in the radiation hardness. The main difference with other Roman Pots designed for other machines lays in the pot technology.

### 4.1.2 The Pot

The pot is a vessel which contains the detectors and keeps them separated from the primary vacuum of the machine. The external surface of the pot is part of the primary machine vacuum, while the internal surface is in the secondary rough vacuum of the detector environment. The detectors are silicon micro-strips mounted on hybrid cards equipped with readout electronic chips. Cooling is provided to evacuate the heat dissipated by the electronics and to stabilize the operational temperature of the silicon not lower than  $\sim 50^{\circ}\text{C}$ .

A flange on the top of the pot makes a connection between the bellows of the primary vacuum chamber the flange closing the pot. This flange has many functions since it deals with the vacuum tightness of the pot, the supports of the detectors and the feed-through of the services.

The detector package has a transverse size of 90mm x 90mm and a depth of 35mm while the active part has an optimized pentagon shape as described in *Figure 4.2*. The detector hybrid cards touch the internal surface at the bottom of the pot, while the active detector



itself is adjusted to be as close as possible (100 microns) from the surface, without touching it.

The pot region close to the beam has a rectangular box shape matching as close as possible the shape of the detector package. The wall thickness is  $\sim 2\text{mm}$ . In the transversal plane a clearance of 30mm on each side of the detector package has to be left for the integration of the supports and the cooling. In the longitudinal plane a clearance of 2.5mm is sufficient.

The total height of the pot is 140mm.

On the rectangular part of the pot, the wall thickness has to be minimized in a region matching the pentagon shape of the sensitive area and the bottom of the pot. The purpose is to reduce the dead space between the beam and the detector and to minimize the amount of material seen by the detector. This part of the pot is called the thin window.

The upper part of the pot, far away from the thin window, must present sufficient space for the electrical connectors, for the cooling and the mechanical mounting.

The pot must be designed with a strength safety factor of 1.5 and all the pots manufactured have to be tested at Ultra High Vacuum before any installation in the machine.

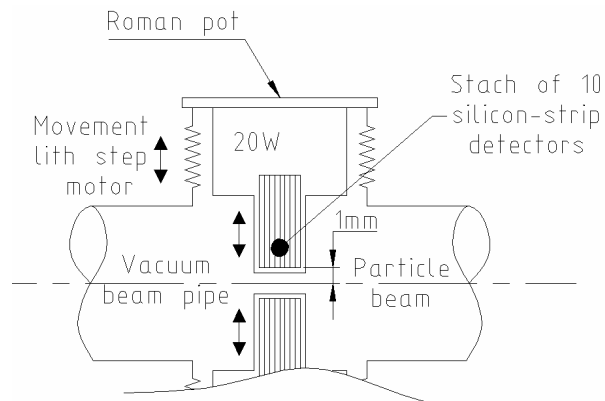


Fig. 4.2 Layout of the LHC-TOTEM



## 4.2 Roman Pot Station

The LHC experiment, TOTEM [6], is designed for measuring the elastic p-p scattering cross-section, the total p-p cross-section and diffractive processes. These physics objectives need the detection of leading protons with scattering angles of a few  $\mu\text{rad}$ , which is accomplished with a Roman Pot (“RP”) system having stations at 147m and 220m from the interaction point 5 where CMS will be located (*Figure 4.3*). Depending on beam equipment integration, each station, composed of two RP units, can be separated by 2.5 to 4m.

Each RP unit contains of a vacuum chamber equipped with one horizontal insertion and two vertical insertions (top and bottom). Each “Pot” insertion is created with a package of 10 silicon detectors in a secondary vacuum. There exists the possibility to move the pots from the secondary vacuum to the primary one of the machine through vacuum bellows. In order to minimize the distance of the detectors from the beam and to minimize multiple scattering, the wall thickness of the pot is reduced to a thin window foil (*Figure 4.4*).

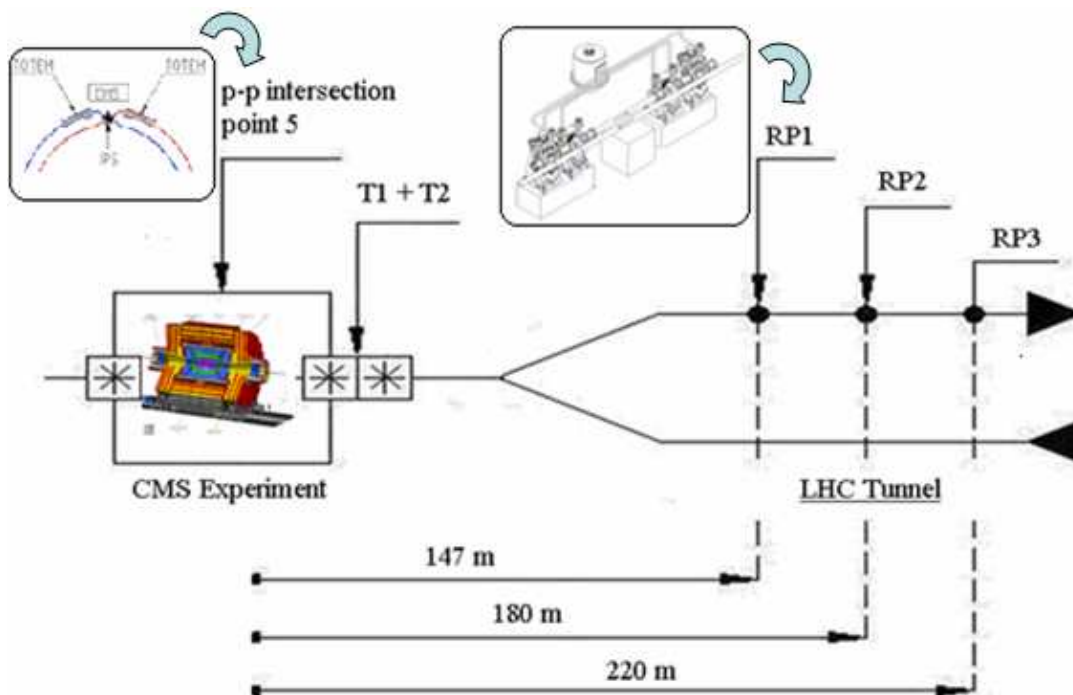


Fig. 4.3 Lay-out of TOTEM



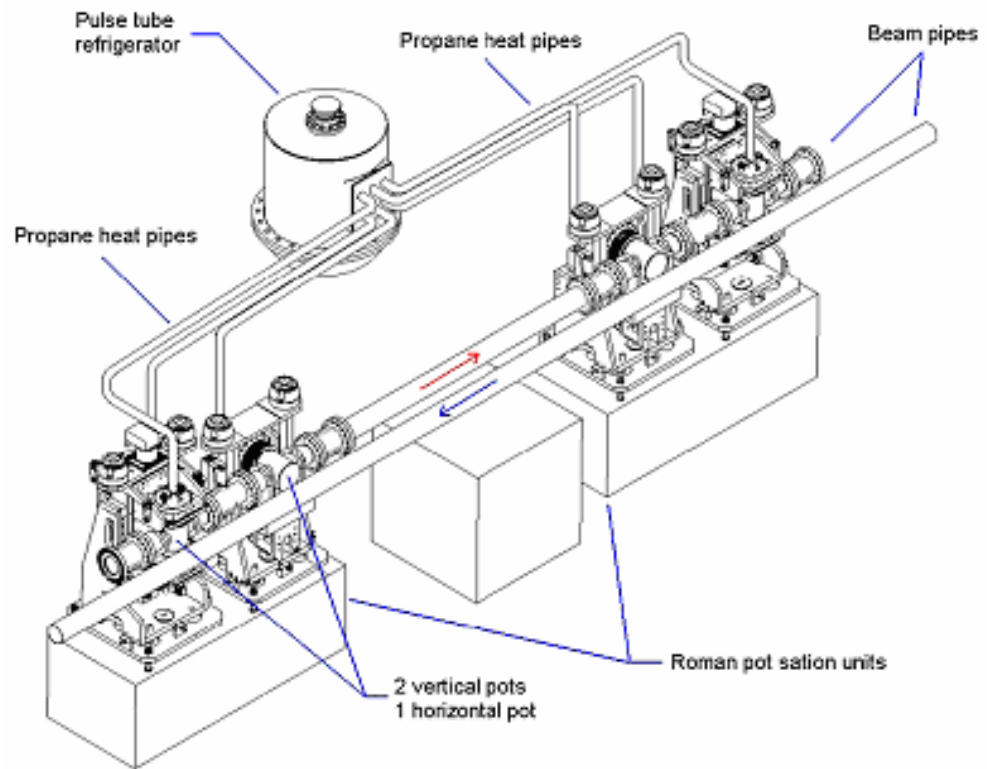


Fig. 4.4 Cooling System lay-out with heat pipes and a central pulse tube refrigerator for an individual roman pot station.



## 4.3 Cooling Proposed

### The Proposed Cooling System

The cooling design concept is based on passive heat transfer with a minimum of active elements. Each of the 2 x 3 roman pot stations (RP1, RP2, RP3) are identically equipped with a modular cooling system consisting of a central pulse tube refrigerator and six heat pipes connecting to the six roman pots. The dissipated heat in each roman pot is collected by thermal contacts and transferred to the outside by conduction through bulk metal to the evaporator of the connected heat pipes.

Each 2.5m long heat pipe transfers the heat to a central cryostat where it is extracted by re-condensation of the working fluid at a heat sink. The cryostat contains the six heat pipe terminals connected to the cold head. The operating temperature is controlled via a film heater attached to the cold head and the excess cooling capacity is dissipated. The refrigerator compressor will be installed in the vicinity of the tunnel. *Figure 4.5* shows the lay-out of a roman pot station with mechanical devices and the modular cooling system.

As the heat pipe principle is based on a self-sustaining continuous evaporation and condensation process of a working fluid with a very effective thermal conductivity, it is well suited to stabilize the temperature of the roman pot connection at a given value even at distance. Operation and transfer of heat starts as soon as a heat source and sink are applied. The heat pipe inner wall is lined with a wick to enhance capillary and radial heat transfer and the temperature gradient in the fluid phase is expected to be 1-2K over its entire length of 2.5m. The pulse tube refrigerator used during the current development phase is based on a design for 165K application [7]. Its cooling capacity is 140W at 130K which can be increased with a larger compressor. Helium is the cycle gas and the operating temperature can be varied from below 100 to 250K which are useful during the development phase.

The heat pipes can be adapted to different temperatures by selecting the appropriate working fluid. The theoretical temperature limits are between the triple and critical point of the respective fluid. However, in practice, operation close to the triple point should be avoided as heat transfer performances are reduced with potential failures due to viscous and sonic limitations of the low density vapour. Close to the critical point the heat of vaporization becomes smaller and boiling becomes a limiting factor for the performance. Further limitations are entrainment and capillary pumping. In table 1, several low temperature working fluids are listed being potential candidates for this application. Furthermore, the overall two-phase cycle pressure drop must be compensated for by the driving capillary and gravitational forces that pump the condensate back to the evaporator. Apart from the fluid properties the geometrical arrangement is of importance. The current design applies longitudinal grooves as a wick structure and the outer pipe diameter is 15 mm. The heat pipe has an average inclination of 5% for gravity to assist in the condensate return flow.

To facilitate the operation of the TOTEM cooling system at different temperature ranges a design feature permits to empty and change the working fluid for adaptation. This is done



with valves installed at the pipe appendix after the condenser allowing the evacuation of the fluid and the refill with a different one.

The design principle will be validated with the installation of a prototype Roman Pot detector unit consisting of a pair of vertical pots at the SPS collider beam in the fall of 2004. Two heat pipes and the above described pulse tube refrigerator will be used for this propose and operation and data acquisition will be done at distance. This permits the verification of the cooling requirements in view of the final installations in 2006. If necessary the refrigerator design may be reviewed for increased cooling capacity.

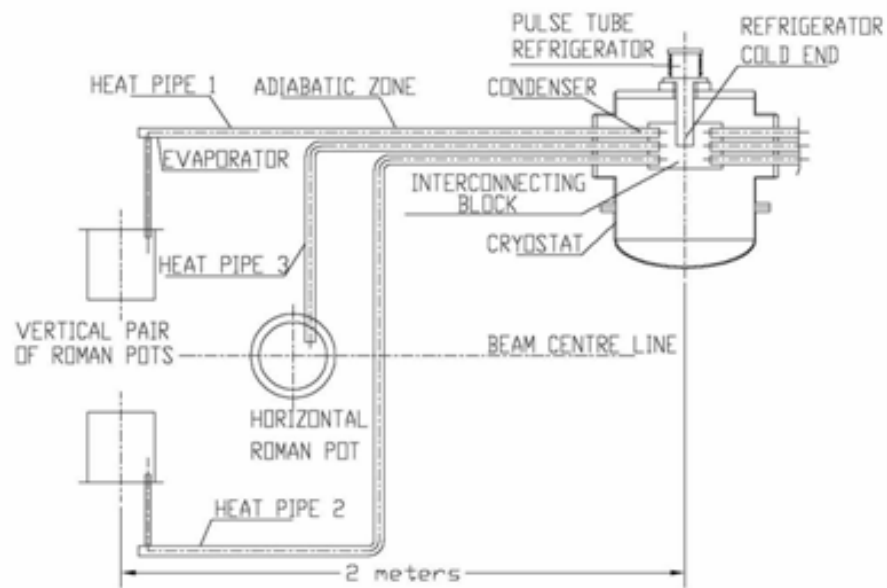


Fig 4.5 System with heat pipes



## 5 Cooling System

### 5.1 Heat Pipes

Heat pipes are sealed vacuum vessels that are partially filled with a working fluid, typically water in electronic cooling, which serves as the heat transfer medium. The heat pipe envelope is made of copper in a myriad of shapes including cylindrical, rectangular, or any other enclosed geometry. The wall of the envelope is lined with a wick structure, which provides surface area for the evaporation/condensation cycle and capillary capability. Since the heat pipe is evacuated and then charged with the working fluid prior to being sealed, the internal pressure is set by the vapour pressure of the working fluid [8].

As heat is applied to the surface of the heat pipe, the working fluid is vaporized (*Figure 5.1*). The vapour at the evaporator section is at a slightly higher temperature and pressure than other areas. This creates a pressure gradient that forces the vapour to flow to the cooler regions of the heat pipe. As the vapour condenses on the heat pipe walls, the latent heat of vaporization is transferred to the condenser. The capillary wick then transports the condensate back to the evaporator section. This closed loop process continues as long as heat is applied.

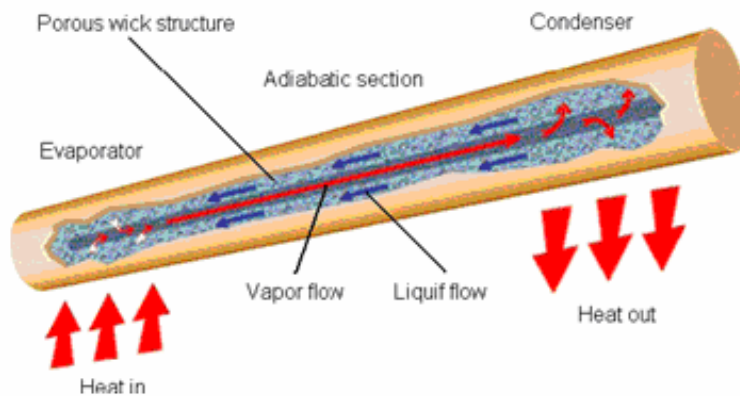


Fig.5.1 Schematic of a heat pipe



### 5.1.1 Theory

In order for the heat pipe to operate, the maximum capillary pumping head  $(\Delta P_c)_{\max}$  must be greater than the total pressure drop in the pipe. There are three components which make up this pressure:

- 1)  $\Delta P_l$ : head required to return the liquid from the condenser to the evaporator.
- 2)  $\Delta P_v$ : head necessary to cause the vapor to flow from the evaporator to the condenser.
- 3)  $\Delta P_g$ : the gravitational head which may be:
  - zero
  - positive
  - negative

$$(\Delta P_c)_{\max} \geq \Delta P_l + \Delta P_v + \Delta P_g \quad (\text{Eq 5.1})$$

Conditions:

- Sonic conditions set one limit to the maximum possible heat transport capability of a heat pipe.
- Low temperatures
- Viscous forces
- ...

The overall performance of the sink is the sum of the individual temperature drops (the theory is given in more detail in *Appendix A.1*) [9]:

$$\Delta T_{Total} = \Delta T_{Block} + \Delta T_{Inter} + \Delta T_{HP} + \Delta T_{Conv} + \Delta T_{Fin} + \Delta T_{Air} \quad (\text{Eq 5.2})$$

The thermal resistance of the sink to ambient is:

$$R_{s-a} = \frac{\Delta T_{Total}}{Q} \quad (\text{Eq 5.3})$$

The above calculation should provide a reasonable estimate on the feasibility of a heat pipe heat sink.

$\Delta T_{Total}$ : Total temperature	$\Delta T_{HP}$ : Heat Pipe Temperature	$\Delta T_{Fin}$ : Fin temperature
$\Delta T_{Block}$ : Block temperature	$\Delta T_{Inter}$ : Intern Temperature	$\Delta T_{Air}$ : Air temperature
$\Delta T_{Conv}$ : Convection temperature	$R_{s-a}$ : Thermal resistance	$Q$ : Heat amount



### 5.1.2 Performance limits

The most important heat pipe design consideration is the amount of power the heat pipe is capable of transferring. Heat pipes can be designed to carry a few watts or several kilowatts, depending on the application. Heat pipes can transfer much higher powers for a given temperature gradient than even the best metallic conductors. If driven beyond its capacity, however, the effective thermal conductivity of the heat pipe will be significantly reduced. Therefore, it is important to assure that the heat pipe is designed to safely transport the required heat load.

The maximum heat transport capability of the heat pipe is governed by several limiting factors which must be addressed when designing a heat pipe. There are five primary heat pipe heat transport limitations. These heat transport limits, which are a function of the heat pipe operating temperature, include: viscous, sonic, capillary pumping, entrainment or flooding, and boiling. *Figure 5.2* shows graph of the axial heat transport limits as a function of operating temperature for typical powder metal and screen wicked heat pipes [10].

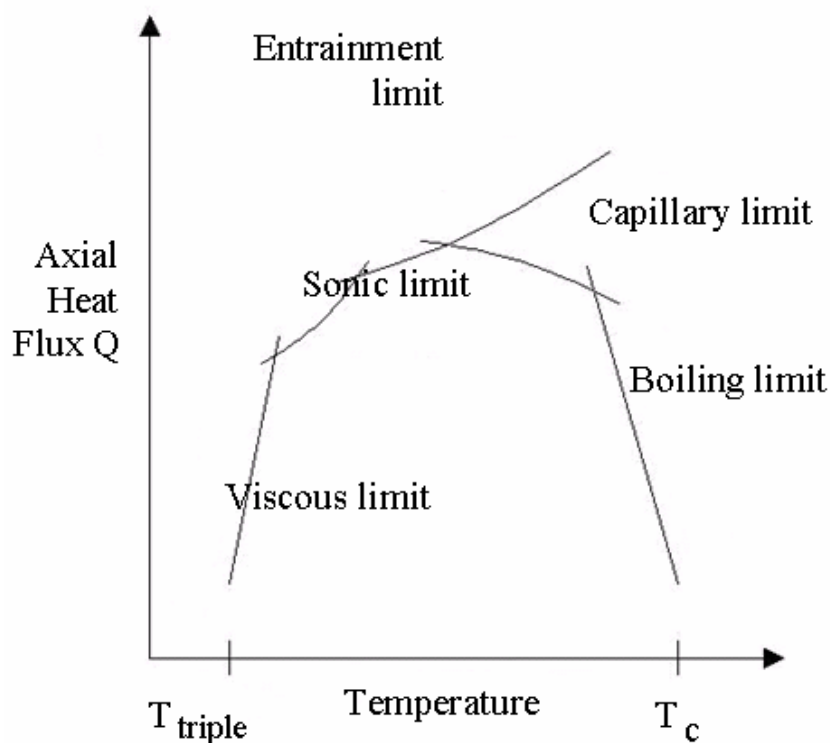


Fig. 5.2 Graphic:  $Q=f(T)$



### Operating limitation:

The operation of the heat pipes is limited by several operating phenomena. Each of these limitations is dependant on:

- Wick structure
- Working fluid
- Temperature
- Orientation
- Size of the heat pipe

The capillary limit is more important than the other limits in our project because the working conditions are normally in range of the capillary limit.

The other limits are mentioned in *Table 5.1*. The parameters of these formulas could be found in *Table 5.2*. More information can be found in *Appendix A.3*.

### Capillary Limit:

The wick structure of the heat pipe generates a capillary pressure, which is dependent on the pore radius of the wick and the surface tension of the working fluid. The capillary pressure generated by the wick must be greater than the sum of the gravitational losses, liquid flow losses through the wick, and vapor flow losses. The liquid and vapor pressure drops are a function of the heat pipe and wick structure geometry (wick thickness, effective length, vapor space diameter, etc) and the fluid properties (latent heat, density, viscosity, etc). A critical heat flux exists that balances the capillary pressure with the pressure drop associated with the fluid and vapor circulation. For horizontal or against gravity (evaporator at a higher elevation than the condenser), the capillary limit is the heat pipe limit. For gravity aided orientations, the capillary limitation may be neglected, and the flooding limit may be used if the heat pipe can have an excess fluid charge.

$$Q_{c,max} = \frac{\frac{2\sigma}{r_c} - \rho_l g d_v \cos \varphi \pm \rho_l g l \sin \varphi}{(F_l + F_v) l_{eff}} \quad (\text{Eq. 5.4})$$



Different performance limits	Formula to calculate the performance limit	
Capillary Limit	$Q_{c,\max} = \frac{\frac{2\sigma}{r_c} - \rho_l g d_v \cos \varphi \pm \rho_l g l \sin \varphi}{(F_l + F_v) l_{\text{eff}}}$	
Boiling Limit	$Q_{b,\max} = \frac{2\pi \cdot l_e \lambda_{\text{eff}} T_v}{h_{fg} \rho_v \ln(r_i / r_v)} \left( \frac{2\sigma}{r_b} - \Delta p_c \right)$	
Sonic Limit	$Q_{s,\max} = A_v \rho_v h_{fg} \left[ \frac{\gamma_v R_v T_0}{2(\gamma_v + 1)} \right]^{1/2}$	
Entrainment Limit	$Q_{e,\max} = A_v h_{fg} \left[ \frac{\rho_v \sigma}{2r_{hs}} \right]^{1/2}$	
Flooding Limit		
Viscous Limit	$Q_{vi,\max} = \frac{d_v^2 h_{fg}}{64 \mu_v l_{\text{eff}}} \rho_{v0} p_{v0} A_{v0}$	
Condenser limitation	For high temperature	$Q_{con,\max} = 2\pi R_0 L_c \varepsilon \sigma (T^4 - T_\infty^4)$
	For low temperature	$Q_{con,\max} = S_c h (T_c - T_\infty)$

Table.5.1 Performance Limits [9]



Symbol of the parameter	Name of the parameter	Symbol of the parameter	Name of the parameter
$\rho_v$	Vapor density	$\phi$	Porosity of wick
$K = \frac{r_s^2 \cdot \phi^3}{37.5(1-\phi)^2}$	Penetration of wick	$p_{c,max} = \frac{2\sigma}{r_c}$	Maximum capillary pressure
$P_s$	Saturation pressure	$F_l = \frac{\mu_l}{KA_w \rho_l h_{fg}}$	Liquid friction
$A_w$	Cross-section surface of wick	$\sigma$	Surface tension
$f_v Re_v$		$\phi$	
$A_v$	Vapor cross section surface	$k_l$	Liquid thermal conductance
$l_a$	Length of adiabatic	$\mu_v$	Vapor viscosity
$l_c$	Length of condenser	$h_{fg}$	Internal energy
$l_e$	Length of evaporator	$\gamma_v$	Ratio of isobaric to isochoric specific heats
$r_{hv}$	Vapor hydraulic radius	$M$	Molar mass
$r_c = 0.41r_s$	Effective capillary radius	$R_0$	Gas constant
$r_s$	Particle radius	$R_v = \frac{R_0}{M}$	
$d_v$	Vapor diameter	$\rho_l$	Liquid density
$d_i$	Inner diameter	$l_{eff} = \left( \frac{l_e}{2} + l_a + \frac{l_c}{2} \right)$	



$\mu_l$	<b>Liquid viscosity</b>	$\lambda_{eff}$	
$F_v = \frac{(f_v Re_v)\mu_v}{2A_v r_{hv}^2 \rho_v h_{fg}}$	<b>Vapor friction</b>	$T_{mel}$	<b>Melting temperature of the working fluid</b>
$T_\infty$	<b>Initial or ambient temperature</b>	$A_w$	<b>Cross-section area of the working fluid in the wick</b>
$r_b$		$C$	<b>Heat capacity per unit length of heat pipe wall and wick</b>

---

Table 5.2 Definition of the parameters



## 5.2 Heat Pipes operation prediction

In order to know the working position of the heat pipe, an experiment was done with different positions of the heat pipe (*Figure 5.3*). The exact positions were: gravity position, horizontal and anti-gravity position. More information can be found in *Appendix A.5*.

### 5.2.1 Gravity Aided:

The evaporator is at lower elevation than the condenser. The Gravity Aided orientation is the most efficient, since the heat pipe acts as a thermosyphon and gravity will return the condenser fluid to the evaporator. Heat pipe operation is typically limited by the flooding limit or the boiling limit. These two limitations are most greatly affected by the diameter of the heat pipe; a larger diameter heat pipe will carry more power.

### 5.2.2 Horizontal:

The Horizontal orientation relies on the wick structure to provide the capillary pressure to return the condensed fluid to the evaporator. The heat pipe operation is typically limited by the Capillary Limit. This limitation is greatly affected by the diameter of the heat pipe (a large diameter heat pipe will carry more power) and the length of the heat pipe (a longer heat pipe will carry less power).

### 5.2.3 Against Gravity:

The evaporator is at a higher elevation than the condenser. Heat pipe operation in the Against Gravity orientation relies on the wick structure to return the condenser fluid up to the higher evaporator. Again the heat pipe operation is limited by the Capillary Limit. This orientation is very similar to the Horizontal orientation, except the effects of gravity must be accounted. A larger elevation difference between the evaporator and the condenser results in a lower power capacity.

All the experiments are done at laboratory (*Figure 5.4*).

In order to understand the operation prediction, a book was used [12]



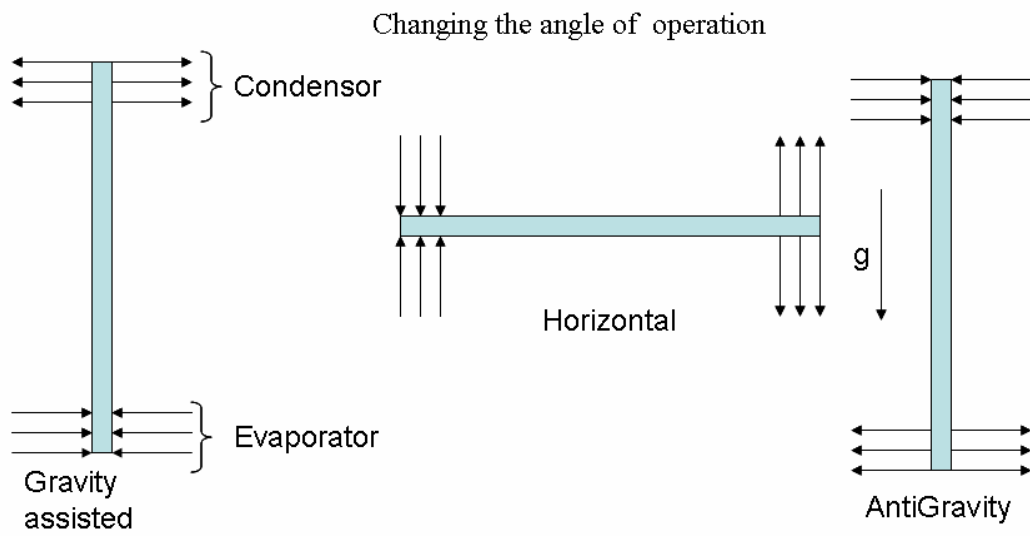


Fig 5.3 changing the angle of operation

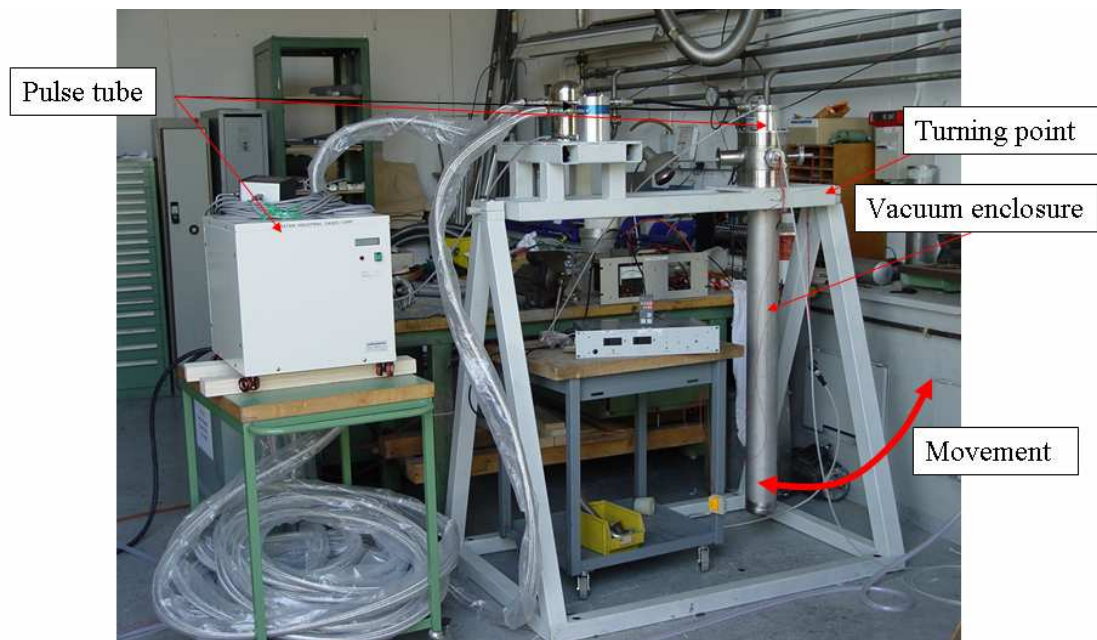


Fig 5.4 Laboratory



## Conclusions

The conclusions after to try the different position, it was the follow ones:

- Gravity assisted the most efficient
- Antigravity the worst
- Gravity helps for 40% of the heat transfer

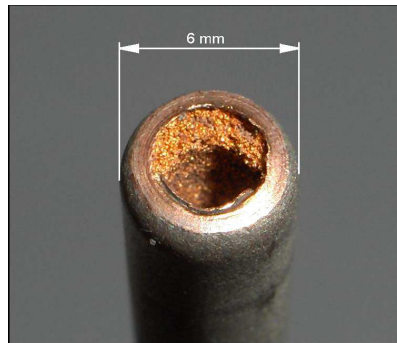
## 5.3 Types of the heat pipes used

The main distinction of heat pipes, besides working fluid, is the wick structure. The capillary structure is the heart of the heat pipes. This is very important, at setups where the condenser is settled below the evaporator and the liquid has to be transported against gravity. Another important task of the wick structure is the surface expansion in the evaporator region. Because of the countless small pores, the surface for the heat transfer between container, wick structure and working fluid is big enough to provide a high heat flow. The wick structure is producing the pressure which is the driving force for the transport of the working fluid. This pressure is increasing when the pore size of the capillaries is decreasing. The pore radius determines the pumping pressure the wick can develop.

The permeability determines the frictional losses of the fluid as it flows through the wick. However, the smaller the pore size, the smaller the wick permeability and the higher the pressure losses in the liquid flow. The most common types of capillary structures are sintered powder, the grooved tube and the screen mesh. Typical sinter powder wick handle  $50 \text{ W/cm}^2$ , and have been tested to  $250 \text{ W/cm}^2$ . In comparison, a groove wick will nominally handle  $5 \text{ W/cm}^2$  and screen wick will nominally handle  $10 \text{ W/cm}^2$ . The two most important properties of a wick are the pore radius and the permeability [13].

The *Sintered Powder* heat pipe is the most efficient heat pipe. Due to the highest capillary pressure it is able to transport large amounts of heat. The disadvantages of sintered powder wick are the high prices for production and the porosity of the wick, which is making a bending of a straight pipe almost impossible (*Figure 5.5*).

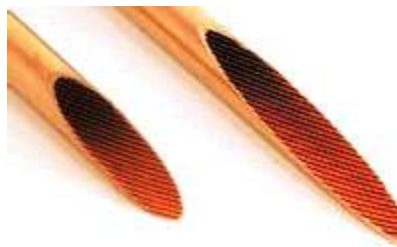




---

Fig 5.5 Sintered wick structure

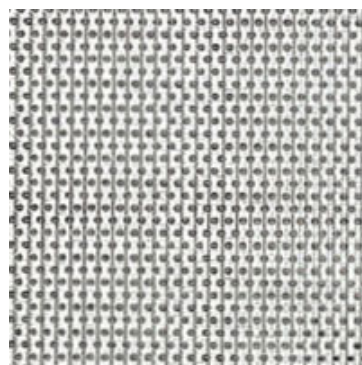
*Grooved tube* heat pipes are suitable for low power applications. The relatively low capillary pressure makes the heat pipes work proper only in horizontal or gravity assisted direction. The big advantage of the grooved tubes is their ability to transport the liquid even when they have several bends along their axes (*Figure 5.6*).



---

Fig 5.6 Grooved tube wick

The *screen mesh* is the mostly used type of wick structure. It is easy to produce and its numerous types of wire thicknesses and pore sizes cover a wide range of possible applications. Sometimes, combinations between these types are also possible. For example the combination of a grooved tube with a screen mesh on the inner wall is widely used (*Figure 5.7*).



---

Fig 5.7 Screen mesh



### 5.4 Working fluid

The criterion which is responsible whether a working fluid can be used in a specific setup or not, is the desired operation vapour temperature. At this temperature, it must be possible to keep vapour and liquid in one system without exceeding a specific pressure range. A second, very important value is the surface tension. The surface tension is responsible for the pressure which is produced in the capillary structure. The higher the surface tension, the higher the pressure gradient which is directly proportional to the maximum pumping height. A proper working fluid must also provide a small viscosity, a high latent heat as well as a high thermal conductivity. The smaller the viscosity in the liquid and the vapour phase, the smaller are the pressure losses in the capillary structure and the vapour line. The latent heat of vaporization is responsible for how many energy can be transported in a certain amount of vapour and a high thermal conductivity provides a more constant radial temperature gradient in the heat pipe. This is very important due to the possibility of nucleate boiling in the wick structure or the container wall when local temperatures become too high. *Table 5.3* shows the thermal gas data from different fluids.

<b>Fluid</b>	<b>Triple point Temp (k)</b>	<b>Critical point Temp (k)</b>
<b>Argon</b>	<b>83.80</b>	<b>150.68</b>
<b>Krypton</b>	<b>115.76</b>	<b>209.38</b>
<b>Xenon</b>	<b>161.36</b>	<b>289.74</b>
<b>Methane</b>	<b>90.69</b>	<b>190.55</b>
<b>Propane</b>	<b>85.47</b>	<b>369.85</b>

Table 5.3 Thermal gas data from different fluids



## 5.5 Application to Prototype Cooling System

To develop heat pipes it was necessary to test them and consequently a test station had to be built.

The purpose of this apparatus was to aid in the process of finding an optimal charging mass of the working fluid and to obtain the maximum heat transfer rate.

The apparatus used for the heat pipes tests was composed of several parts which are now described from top to bottom. On top was placed the pulse tube refrigerator that cools the heat pipes - the condenser. Connected to this was a copper block adapter that could be changed depending on the outer diameter of the heat pipe to be tested. The heat pipe was then pressed between the two copper block parts in order to obtain maximum thermal contact. Temperature sensors were placed along the heat pipe in order to allow the measurement of temperatures. At the opposite edge of the heat pipe to the copper block adapter another copper block, this time parallelepiped, was placed around the heat pipe. Glued to two opposite sides of this one were two film heaters that allowed inputting heat into the heat pipe extremity - the evaporator (*Figure 8*).

To permit the filling of the heat pipe without having to remove it from the apparatus each time that the procedure was necessary, a small diameter copper tube was connected to one end of the heat pipe leading to the working fluid container, with some valves in the middle to control the passage of the fluid.

All of this described above was inside a vessel that was vacuum sealed.

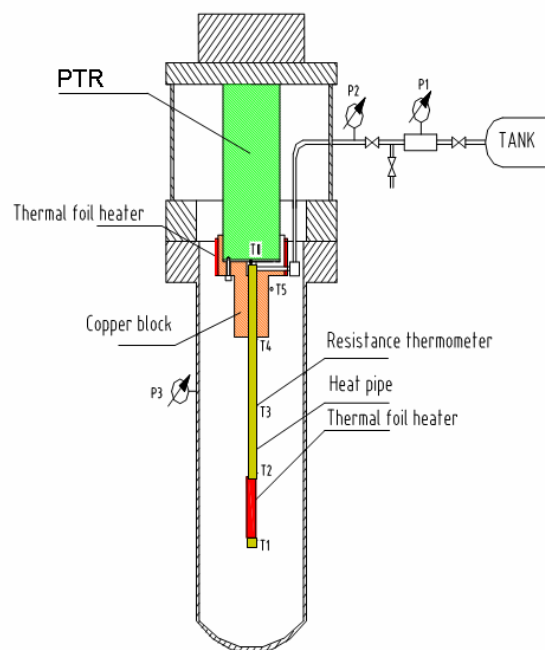


Fig 5.8 apparatus to measure the Heat Pipe



## 5.6 Loop Heat Pipes

In parallel to the testing of the Thermal Model and its heat pipes, a second study was started. In this study, the use of so-called loop heat pipes for cryogenics and the Thermal Model should be evaluated. For this purpose, different loop heat pipes should be designed and tested under various conditions.

The first loop heat pipe was developed in 1972 by the Russian scientists Gerasimov and Maydanik from the Ural Polytechnical Institute. It had a length of 1.2m and was able to transport 1kW of heat. A loop heat pipe basically works the same way as a common heat pipe. The main difference is that the system has separated vapor and liquid lines and accompanied with that fact only one flow direction. Moreover, the capillary structure is only located in the evaporator region. This reduces friction losses in the adiabatic zones and the condenser.

### 5.6.1 Technical conclusion

Loop heat pipes refer to the low temperature devices with the use of a working fluid with a relatively low value of the surface tension coefficient.

The right combination between wick material, pipe material and working fluid is the key for the high functionality of the heat pipe. The most used materials for the wick are sintered nickel, copper or titanium parts, with pore radii between 0.7 $\mu\text{m}$  and 15 $\mu\text{m}$ .



## 5.7 Pulse Tube

### Set up for testing heat pipes at low temperatures

A pulse tube refrigerator is a device for cooling to low temperatures (*Figure 5.9*). It is a closed system that uses an oscillating pressure at one end (typically produced by a compressor) to generate an oscillating gas flow in the rest of the system. This gas flow, usually helium gas, can carry heat away from a low temperature point, cold heat exchanger, if the conditions are right [14].

A single pulse tube refrigerator can cool from room temperature to 30 K and multi-stage systems can cool much lower. Their efficiency is comparable to other systems such as Stirling coolers and GM coolers

The primary advantage of pulse tube coolers over Stirling coolers and GM coolers is that they have no moving parts in the low-temperature region. This means that there is much less friction, wear and essentially vibration, so the low-temperature sections have much longer lifetime.

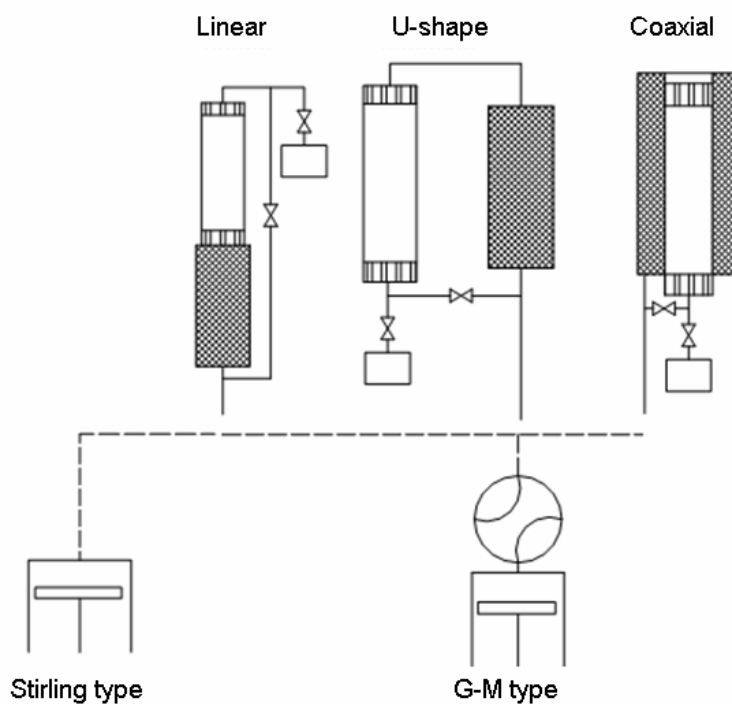


Fig 5.9 Pulse tube refrigerator

For the cooling effect in the tube the source of the pressure variations is unimportant. As long as there are pressure variations there is cooling. In practice two ways to obtain the pressure oscillations are used.



## **Stirling type versus GM type [15]**

### **Stirling**

In the so-called Stirling-type PTRs a piston is directly coupled to the hot end of the regenerator. The frequency of the compressor is the same as of the pulse tube. The power, supplied to the compressor, must be removed as heat to the environment by a heat exchanger between the compressor and the entrance of the regenerator. These aspects are the same as in Stirling coolers. Stirling type of PTRs is used in the temperature range of about 50 K and higher. Typically the driving frequency is 25 to 50 Hz.

### **GM**

PTRs for lower temperatures (20 K and below) usually operate at low frequencies (1 to 2 Hz). At room temperature the swept volume per cycle would be very high (up to one liter and more). Therefore it is more practical to uncouple the compressor from the cooler. Now the compressor runs at high frequency (50 Hz) which leads to a reduced compressor volume. The cooler frequency is uncoupled from the compressor frequency, so the two subsystems can be optimized independently. The compression heat is removed by cooling water in the compressor. The compressor delivers a constant high pressure and a low pressure

A system of valves is needed, which alternatingly connects the high pressure and the low pressure to the hot end of the regenerator. The high-temperature part at the compressor side is the same as in GM-coolers. Therefore this type of PTR is called a GM-type pulse-tube refrigerator. The gas flows through the valves are accompanied by losses which are absent in the Stirling-type PTR. Therefore the GM-type PTR usually is less efficient than the Stirling type.

### **Various shapes**

#### **Linear**

PTR.s can be divided according to their shape. If the regenerator and the tube are in line (as in Fig) we talk about a linear PTR. The best arrangement for mounting the PTR in the vacuum chamber is with the hot end of the tube, where heat is released to the environment, connected to the vacuum chamber wall and the hot end of the regenerator inside the vacuum chamber.

#### **U-shape**

The disadvantage of the linear PTR is that the cold region is in the middle of the cooler. For many applications it is preferable that the cooling is produced at the end of the cooler. By bending the PTR at the cold end of the regenerator and the tube we get a U-shaped cooler. Both hot ends can be mounted on the flange of the vacuum chamber at room temperature. This is the most common shape of PTR.s.



## Coaxial

For some applications it is preferable to have a cylindrical geometry. In that case the PTR can be constructed in a coaxial way so that the regenerator becomes a ring-shaped space surrounding the tube. A disadvantage of this construction is that there is thermal contact between the tube and the regenerator. Generally the two temperature distributions differ. This leads to heat exchange which results in a degradation of performance. Especially the hot end of the tube can become really hot (up to the melting temperature of soft solder). This means that the gas, entering the regenerator, is heated by the hot end of the tube.

The main components of PTR include cold and hot heat exchangers, a regenerator, a pulse tube, orifices and a reservoir

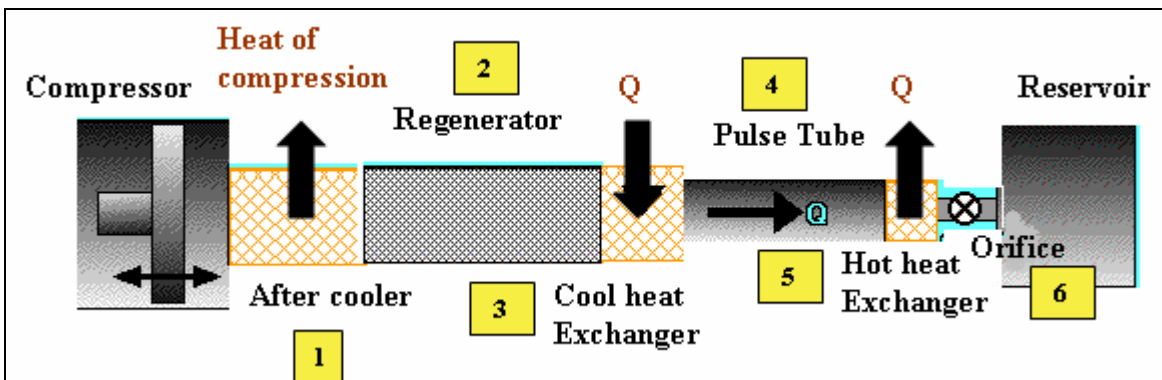


Fig 5.10 Schema of the Pulse tube

- (1) The **after cooler** is a copper heat exchanger that removes the heat of compression so that the regenerator can work more efficiently.
- (2) The **regenerator** is a kind of heat exchanger that provides a way to get the gas to the low temperature region with as much potential work (cooling power) as possible without carrying a lot of heat with it. It doesn't put heat in or out of the system but it absorbs heat from the gas on one part of the pressure cycle and returns heat to the gas on the other part.
- (3) The **cool heat exchanger** is the coldest point of the system; it is here that heat is put into the system from the load to be cooled.
- (4) The **pulse tube** section provides a way for the gas flow to do its cooling; if there is a suitable phase relationship between the pressure and the gas flow in the pulse tube, then heat will be transported from the cold end to the warm end (*Figure 11*).
- (5) The **hot heat exchanger** is used to remove the heat carried through the pulse tube section from the cold end.
- (6) The **orifice** and the reservoir work together to provide that phase shift. With proper



design, the heat flow can be made quite large. In practice, the orifice is replaced by an iteration tube.

In our laboratory, there is a high power coaxial GM-type pulse tube refrigerator. It provides a cooling power of 70 W at 165K by using a 2.2 kW GM-type compressor (*Figure 5.12*).



---

Fig 5.11 Rotary valve + Cold Head



---

Fig 5.12 Compressor



## 5.8 Radiation Environment

The detectors of the Roman Pot stations are high precision tools in a radiation zone. Thus, the cooling system and the Pots have to be maintenance free without any mechanical and electrical failures. Active cooling systems are cheap and have a high heat transfer rate in comparison to heat pipes, but the vibrating fluid flow and the electronics make the use in the radiated tunnel impossible. Thus, the choice was made for the passive cooling heat pipes.

The radiation level in the tunnel may have consequences on the Roman Pot equipment and its ancillary equipments. As a general consideration, all the components containing plastics, like the motor winding, part of the cooling plant, services and connections may be affected by the absorbed radiation dose, integrated over full operation of LHC. Those components are equally exposed to radiation even when the Roman Pots are not operated and kept in the garage position.

As the working temperature of the detector in the Thermal Model is fixed to 220K, a suitable working fluid for the heat pipes had to be found. The working temperature range of a fluid is limited by two values. The minimum working temperature is given by the temperature at the triple point and the maximum working temperature is restricted by the critical point of the gas. For 220K, most Freon's or other refrigerants would be the best solution, as they have a high thermal conductivity. However, the radiation of the LHC proton beam would destroy the fluid. The weak bindings between the atoms in the molecule would break and free radicals would form new materials. To be sure about the effect of hard  $\beta^-$  radiation on the working fluid, a study was conducted. In the tests, heat pipes with 3 different working fluids were radiated with 60°C and a total dose of 0.9MGy.

This dose is equal to 10 years of radiation in the LHC beam pipe. The tests showed that the propane and methanol heat pipes lost their ability to transport heat. The Xenon as an inert gas showed no realizable changes. The big disadvantages of the Xenon are its high price from about 20 CHF per gram and its high liquid density of 2.5kg/dm<sup>3</sup>. For this reason, a design was chosen, which provides a good performance and a resistance against hard  $\beta^-$  radiation, using minimum amounts of Xenon.

Inside the high radiation zone, four small Xenon heat pipes with 6mm in diameter transport the heat to a connector. The connector is a round tube which contains the condenser region of the Xenon heat pipes and the evaporator region of a Propane heat pipe. The connector is flooded with liquid Cerrobend ®, a woods alloy which is melting at 74 °C. This guarantees a good thermal contact between the heat pipes and mechanical strength as support. This design provides resistance against radiation and maximum performance by using the Xenon only in the radiation infected zone.

For more information about the analysis used to conclude with the above explications refer to *Appendix A.5*



## 5.9 Conclusions

After performing all tests, where working characteristics were changed each time, such as, dimensions of the heat pipes, kind of heat pipes, working fluid, power applied, wick structure, disposition of the test (gravity assisted, horizontal or anti-gravity), it was concluded that for the Thermal Model experiment the kind of heat pipes that could be used were the ones represented in the *Table 5.4*.

Kind of Heat Pipe	Wick Structure	L (mm)	Ø (mm)	Working fluid	Quantity to fill (g)	Power (W)
Small	Mesh	300	6	Xenon	3.5	30
Big	Groove	950	12.7	Propane	5	50 (*)

**(\*) Maximum heat transfer rate up to 80 W in a gravity assist.**

---

Table 5.4 Conclusion of the Heat Pipes



## 6 Prototype Cooling System and Roman Pot Thermal Model

The thermodynamic objective of the project entitled, "Thermal Model", is to extract the heat released by the detector when the beam passes through it and to establish an average temperature suitable for safe operation of the various detector components.

TOTEM seeks to make measurements of the particles scattered from the CMS collision point at small angles around the LHC beam axis. Therefore, the beam referred to in this project is *not* the LHC beam, but rather the flux of these scattered particles which TOTEM seeks to measure.

Each Thermal Model is located into the Roman Pot. The *Figure 6.1* shows the sequence of the parts from the TOTEM to the Thermal Model.

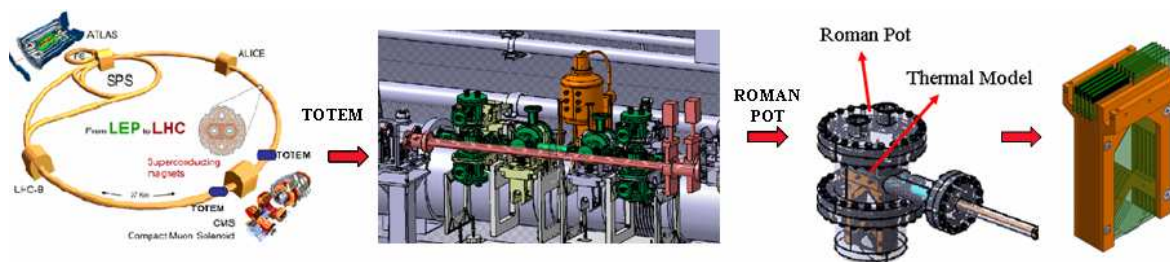


Fig 6.1 Sequence of the parts from the TOTEM to the Thermal Model

The purpose of the Thermal Model is to keep the whole support around the detectors on a working temperature of 220K. Deviation from this temperature would lead to a deformation of the support and thus to a movement of the high precision detectors. The heat which has to be transported is produced in electronics around the silicon detector. This heat will not exceed 20W per Thermal Model. It is transported through heat pipes to a pulse tube refrigerator which is providing the heat sink for this exchange (*Figure 6.2*).

The Thermal Model (*Figure 6.3*) consists of 10 copper frames which carry the PCB cards for the electronics and the detectors. These 10 frames and additional two top frames are screwed together to a stack. This provides a good thermal transport of heat from the detectors to 4 Xenon heat pipes placed in the top frames.



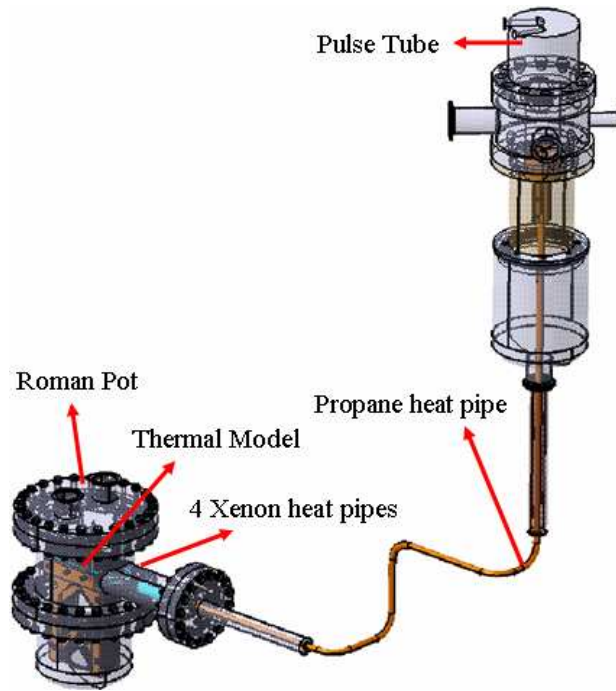


Fig 6.2 Picture of all the system

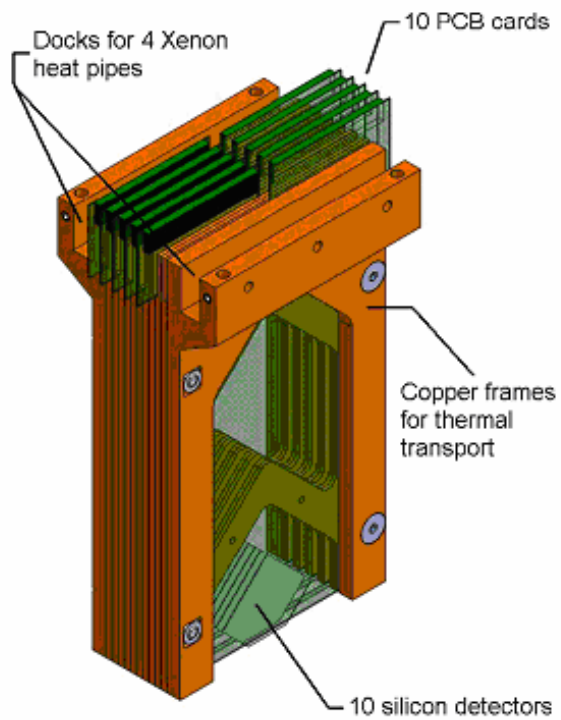


Fig 6.3 Thermal Model



## 6.1 Planning

During the phase of the project planning, the goals of the project were set and an approximate diagram was developed. The goal is to simulate the future conditions of the Thermal Model and to evaluate, based on the research, if and how the Thermal Model is useful as a cryogenic cooling system. The test setup has to be developed so the main tasks are to create a prototype of the model and to find the correct instrumentation for taking the data. To specify the test conditions, the working temperature should be around 220K.

The first step was to conduct a wide-range study about the principles of the thermodynamics of the Thermal Model. Based on the literature studies and calculations, a preliminary design of the Thermal Model was planned and pieces were designed. The designs were sent to the workshop and the pieces manufactured. Since the objective was to know the temperatures and the strain in several points of the Thermal Model, proper instrumentation to measure these characteristics was ordered. Assembly of the Thermal Model was made following the arrival of all the composing pieces and instrumentation. After completing the assembly, thermodynamic and mechanical tests were performed during which the desired data was acquired using LabView software developed for this purpose. The final step was to analyze all the stored data and to propose modifications to the prototype model in order to improve it.

All these values and decisions led to the project definition (*Figure 6.4*) and the project Timetable (*Table 6.1*).

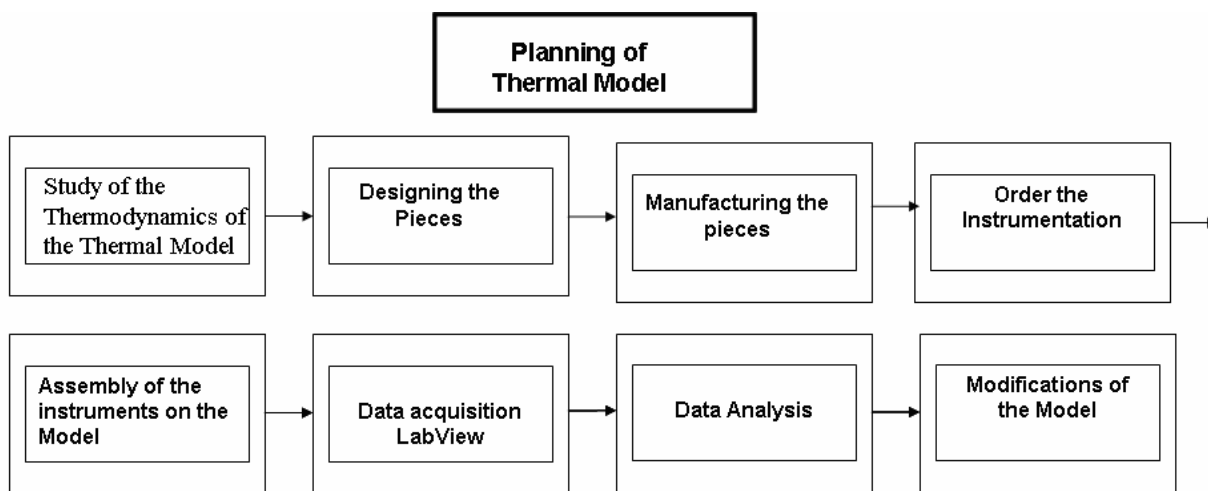


Fig 6.4 Planning of the Thermal Model



<b>☐ Thermal Model</b>	<b>228 days</b>	<b>Wed 6/1/05</b>	<b>Fri 4/14/06</b>
Documentation about thermodynamic systems	12 wks	Wed 6/1/05	Tue 8/23/05
Pieces's shape was dicussed with the designer	4 wks	Wed 6/1/05	Tue 6/28/05
Structure and assembly were determinated	0 wks	Tue 6/28/05	Tue 6/28/05
Fabrication of the pieces	8 wks	Wed 6/29/05	Tue 8/23/05
<b>☐ Planning and Management</b>	<b>228 days</b>	<b>Wed 6/1/05</b>	<b>Fri 4/14/06</b>
Electronics	40 wks	Wed 6/1/05	Tue 3/7/06
Deformation (Strain Gauges)	28 wks	Mon 10/3/05	Fri 4/14/06
Design	4 wks	Wed 6/1/05	Tue 6/28/05
Radiation (Peltier and Heat Pipes)	4 wks	Thu 9/1/05	Wed 9/28/05
Decide which type of Heat Pipe will be use	0 wks	Mon 8/1/05	Mon 8/1/05
Organize all the instrumentation for the tests (temperatures and deformation)	28 wks	Wed 6/1/05	Tue 12/13/05
<b>☐ Software to control the temperatures (LabView)</b>	<b>41 days</b>	<b>Mon 10/17/05</b>	<b>Mon 12/12/05</b>
Learn the program	8 wks	Mon 10/17/05	Fri 12/9/05
Creat the program with this software	6 wks	Tue 11/1/05	Mon 12/12/05
Assembly	0.5 wks	Mon 1/16/06	Wed 1/18/06
Test of the Thermal Model	12 wks	Wed 1/18/06	Wed 4/12/06
Modification on the Thermal Model	12 wks	Wed 1/18/06	Wed 4/12/06

Table 6.1 Project timetable



## 6.2 Designing the Model

### Size limitations

The design of the Thermal Model had to take into consideration dimensions and radiation because it would be placed in the LHC experiment and subject to fixed rules and requirements of the sizes.

From top to bottom was placed the piece with two feedthroughs. One of these allowed the passage of the wires and the other one the vacuum system. Between the detector assembly and the piece with the feedthrough were four standard flanges whose main function was to keep all the pieces. The material of these flanges was stainless steel in order to stop the transfer of heat from the detector assembly to the top.

The detector assembly with support structure consisted of 12 copper frames as mechanical support for the 10 PCB cards and for bud heat conduction. The frames and cards were equipped with heaters, temperature sensors and strain gauges to simulate the load. The model used heat pipes to conduct the dissipated heat to a refrigerator. The copper bridge on the cards was used to take the heat from the detector and to transfer it to the copper frames towards the heat pipes system.

The copper rings were used to connect one piece to the other one.

Afterwards, the top vacuum vessel was placed. The dimension of this piece was decided on by the designer of the TOTEM group. To optimize the height of the pieces to place in the Roman Pot, the race-track shape was used. Into it, there was two blocks that kept the four heat pipes in their place. This block helps to have a good conductivity.

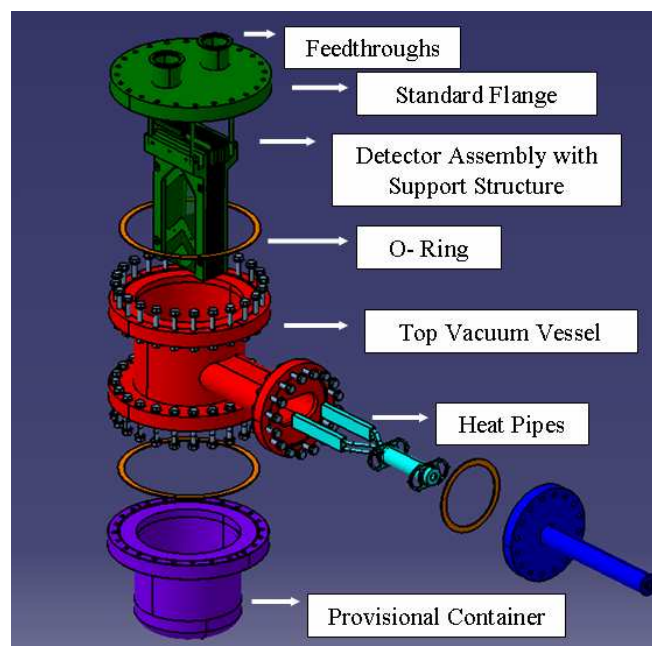


Table 6.5 Design of the Thermal Model

### 6.3 Temperature sensors location of the Thermal Model

The main objective of this study is to carry out a thermodynamical analysis of the Thermal Model's behaviour.

The Thermal Model consists of many parts, one of them composed by the silicon detector and the electronic components adjacent to it. The final design of this electronic part was not yet finished meaning that to carry out this thermodynamical study it was decided to use instead of some electronic elements some film heaters in order to simulate the power loss of the former when the beam passes through the detector.

In totally, there were placed 10 heaters, one in each PCB card, in the future position of the electronic components. Since it's expected that the heat loss will not overcome 20 watts, the maximum power that each heater is allowed to apply is 2 watts.

The idea to place the temperature sensors along the copper frame is to get to know the heat conduction from the bottom, where the detectors are, to the top, where the heat pipes are placed (*Figure 6.6*). There were 8 temperature sensors on these sites.

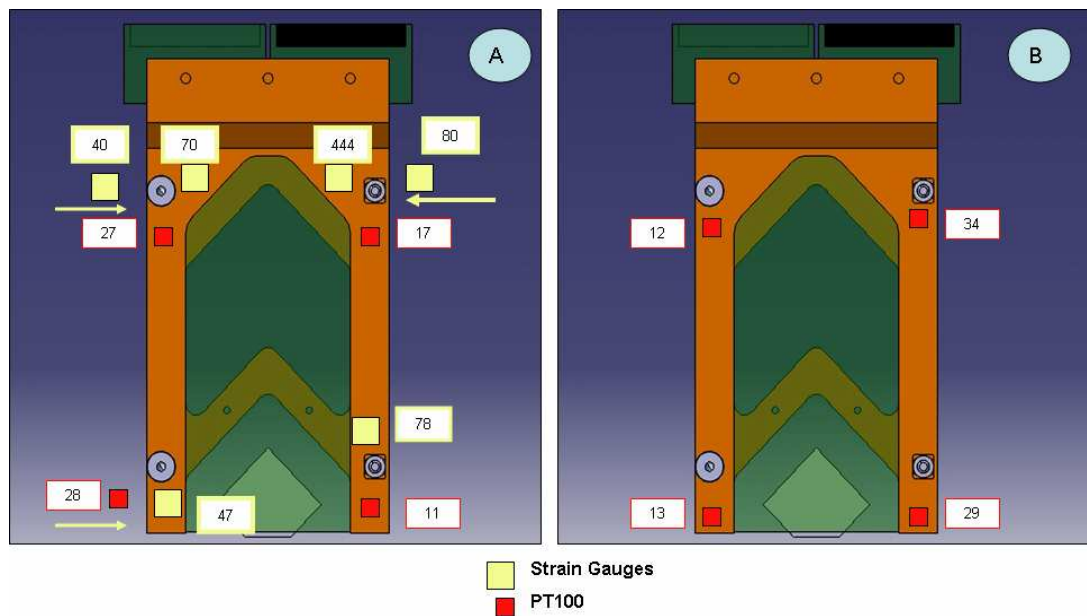


Fig 6.6 temperature sensors location on the frame



Six temperature sensors were placed on both sides of the copper frame, in order to know the temperature gradient (*Figure 6.7*).

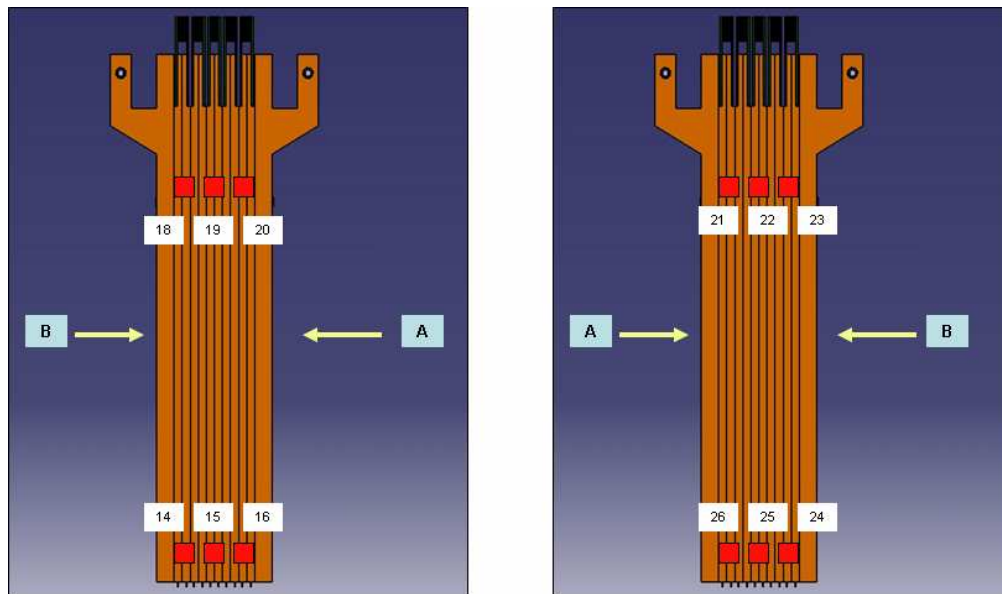


Fig 6.7 temperature sensors location on the both sides of the copper frame

In order to control the temperature of the heat pipes it was placed 4 temperature sensors on the top of the prototype (*Figure 6.8*).

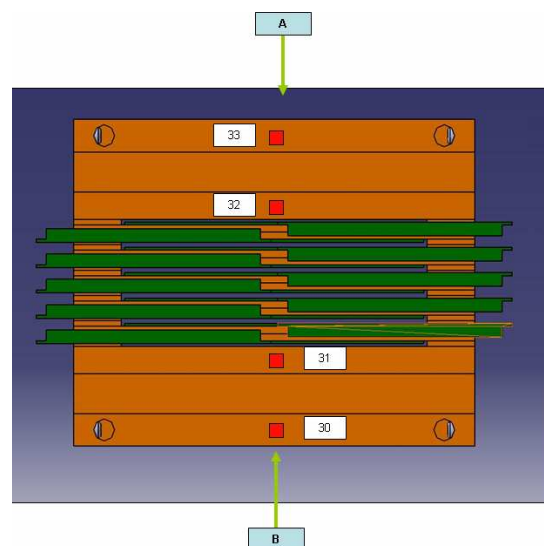


Fig 6.8 temperature of the Heat Pipes



The placement of the temperature sensors on the PCB cards should be on the second, fourth, sixth, eighth and tenth. The last one has 3 temperature sensors. They were placed near where the edge of the silicon detector would be glued on since it is the place where the beam passes through (*Figure 6.9*).

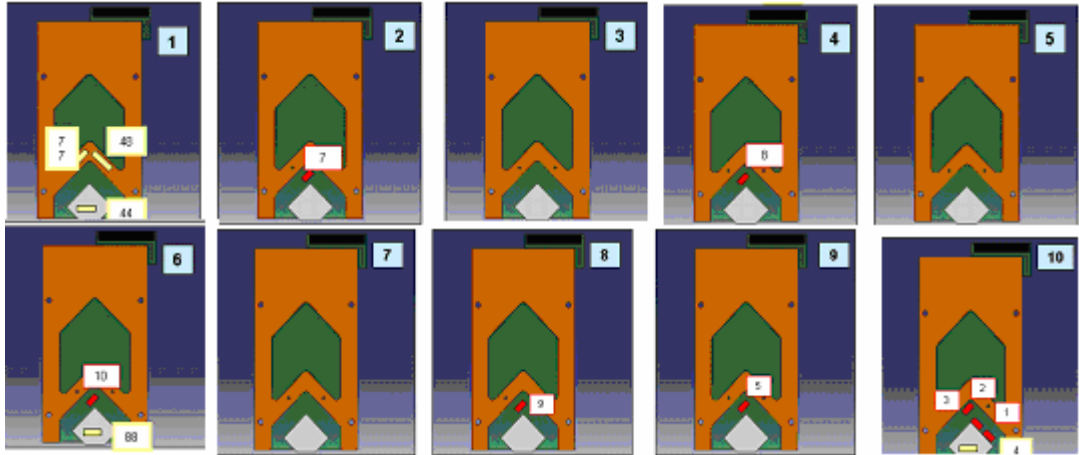


Fig 6.9 temperature sensors location on the cards

Considerations taken into account while installing the PT100:

In order to simulate the electronics, it was used Filmed Heaters on the prototype, and this way it can be simulated the heat that will be generated during the experiment.

It took several days in order to precisely install all the electronics, including the PT100 sensors and the Filmed heaters (*Figure 6.10*).

Due to the fact that these sensors are very delicate, we must follow a precise installation procedure: first the location for the PT100 was marked on the frame; Afterwards the surface was cleaned with an epoxy alcohol and the sensors were glued with Antracita®. Finally the PT100 had remain compressed for one day in order to dry and attach in conformity to the copper / PCB plates.-



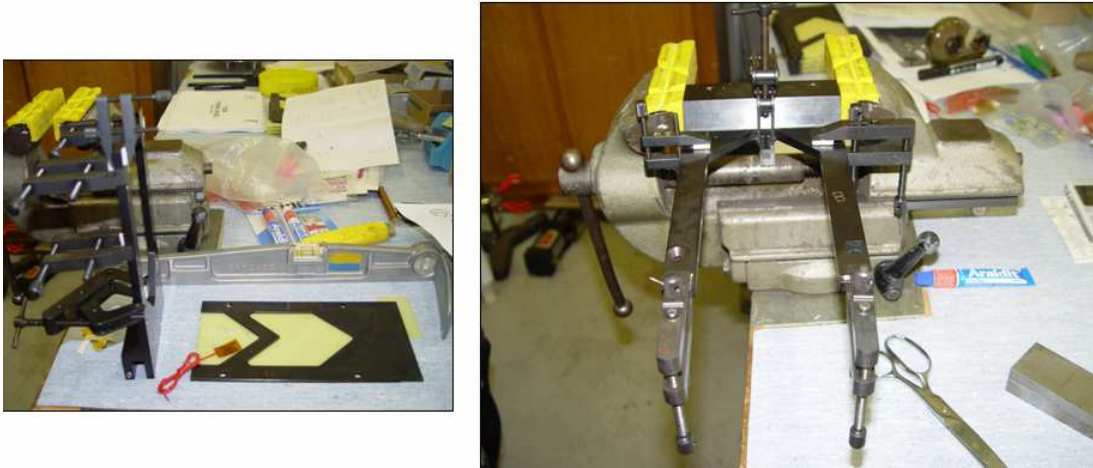


Fig 6.10 Gluing PT100 and Heaters

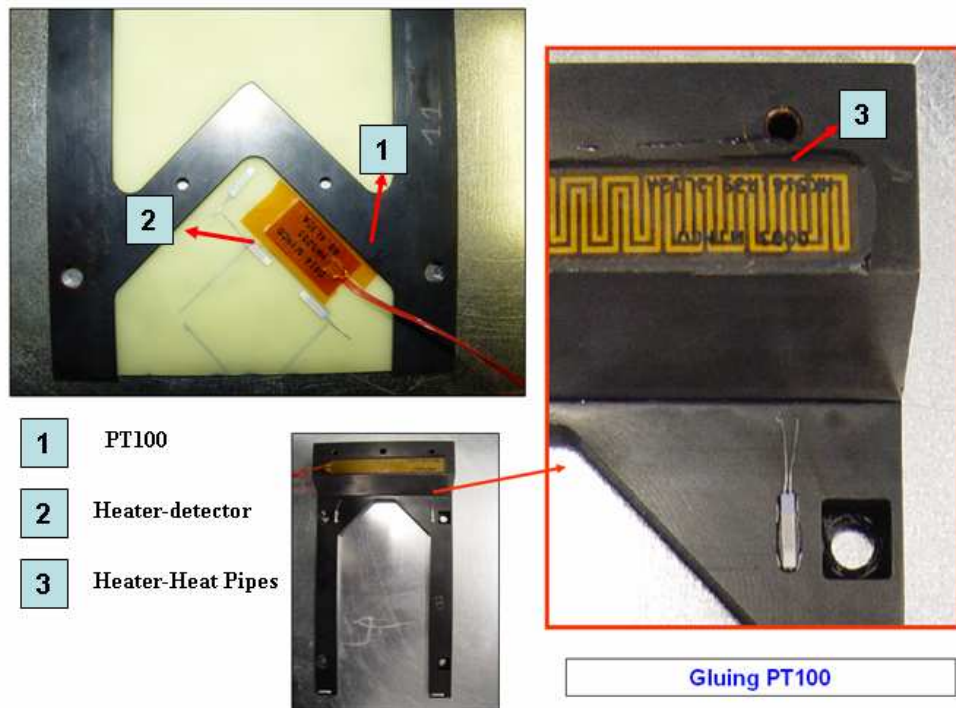


Fig 6.11 Detail pictures of the heaters and the PT100



## 6.4 Mechanical study of the Thermal Model

The mechanical study of the Thermal Model has been carried out by another member of our group but I followed his work because we worked in parallel all the time. Most of the ANSYS Graphics about the temperatures around the model has been discussed together. The strain gauges compliment the thermo-dynamical results.

Strain is the amount of deformation of a body due to an applied force. More specifically, strain ( $e$ ) is defined as the fractional change in length, as shown in (*Figure 6.12*) below.

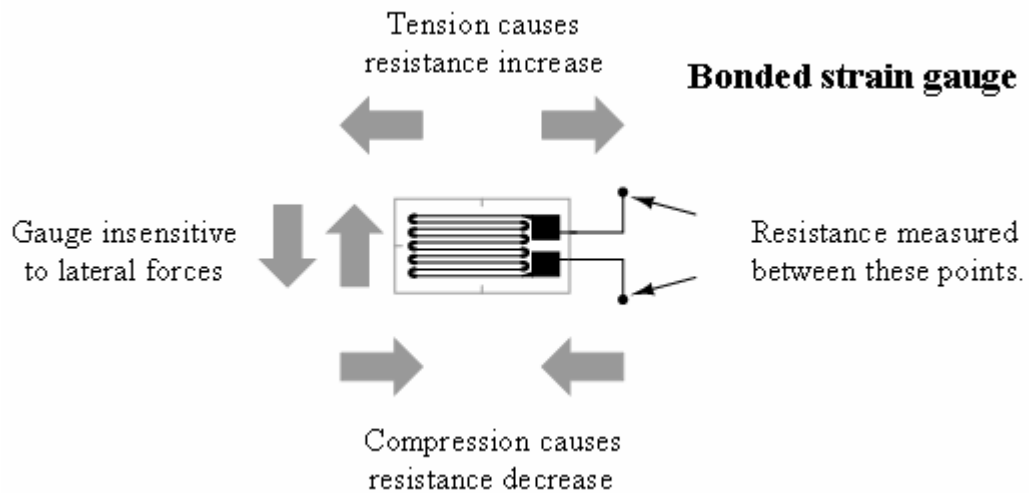


Fig 6.12 Schema of the Strain Gauge

Strain can be positive (tensile) or negative (compressive). Although dimensionless, strain is sometimes expressed in units such as in/in. or mm/mm. In practice, the magnitude of measured strain is very small. Therefore, strain is often expressed as microstrain ( $\mu\epsilon$ ), which is  $e \times 10^{-6}$ .

While there are several methods of measuring strain, the most common is with a strain gauge, a device whose electrical resistance varies in proportion to the amount of strain in the device.

The metallic strain gauge consists of a very fine wire or, more commonly, metallic foil arranged in a grid pattern (*Figure 6.13*). The grid pattern maximizes the amount of metallic wire or foil subject to strain in the parallel direction. The cross sectional area of the grid is minimized to reduce the effect of shear strain and Poisson Strain. The grid is bonded to a thin backing, called the carrier, which is attached directly to the test specimen. Therefore, the strain experienced by the test specimen is transferred directly to the strain gauge, which responds with a linear change in electrical resistance [16].



It is very important that the strain gauge be properly mounted onto the test specimen so that the strain is accurately transferred from the test specimen, through the adhesive and strain gauge backing, to the foil itself.

To corroborate our simulated conclusions, it will be locally place strain gages in all the critical areas which will allow us to obtain real-time and precise values of the strain that the cards will sustain during operation [17]. In totally there will be 11 Strain Gauges on the Thermal Model (*Figure 6.14*).

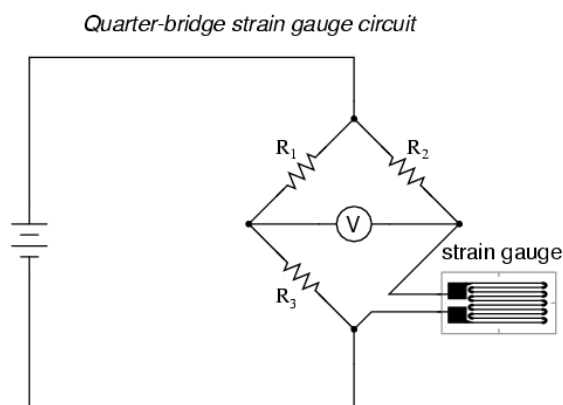


Fig 6.13 Strain gauges 350 ohm GF: 2.01

For this experiment it was used the following strain gauges manufactured by HBM:

**HBM - 1 – L C 1 1 – 6 / 350**

1	<b>standard cables</b>
L	<b>One measuring grid, linear strain gage</b>
C	<b>Carrier and cover for specified temperature range</b>
1	<b>Layout of grids</b>
1	<b>Temperature compensation</b>
<b>6</b>	<b>Measuring grid length (mm)</b>
<b>350</b>	<b>Measuring grid resistance (ohms)</b>

Table 6.2 characteristics of the HBM strain gauges



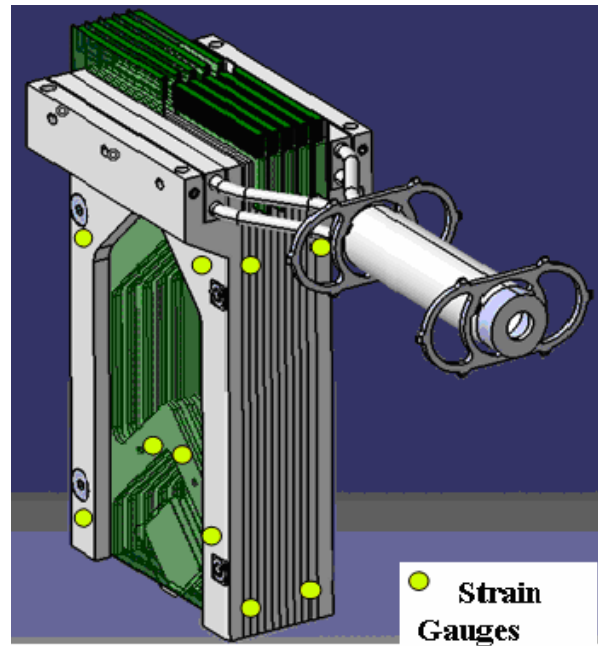


Fig 6.14 Strain Gauges location

It was also able to simulate the strain with ANSYS software [18], but to ensure accurate results there is no comparison to real time measurements in the laboratory.

In order to calculate the thermal strain that will occur on the model, an ANSYS simulation will be carried out.

- We will search for critical areas and any signs of buckling from the PCB cards.
- The first card and plate will be individually simulated, followed by a complete 10 card simulation.
- A transient analysis will also be studied.

The strain gauges were placed in the most critical areas, and applied primarily in the YY direction where it was assumed that the deformation would be the most profound. On the symmetrical side it would be measured the deformation in XX, and in the middle of the frame it would be measured both axes simultaneously.



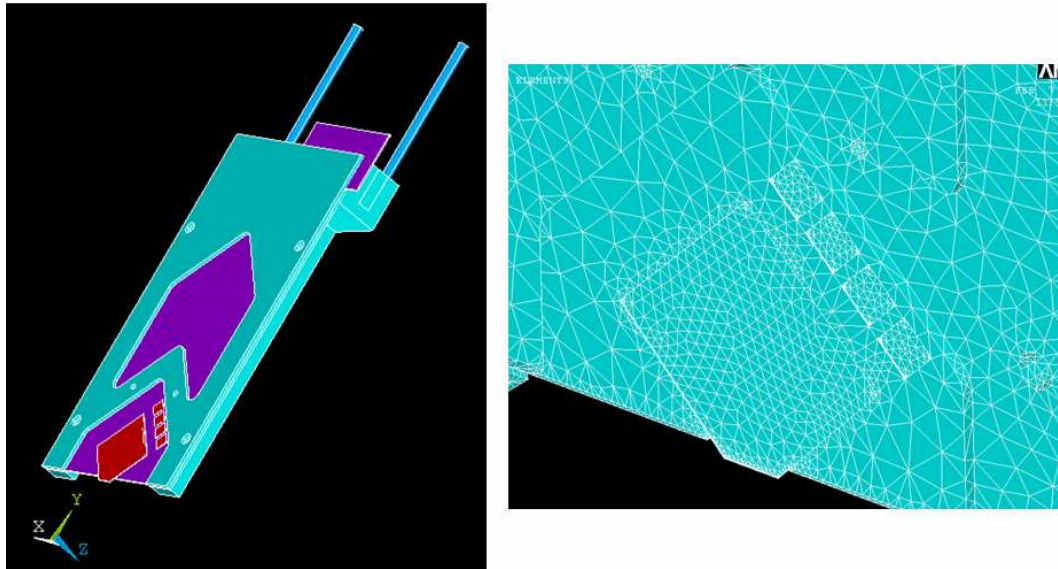


Fig 6.15 Mesh structure (ANSYS)

Initials Assumptions:

- Copper Frame ideal temperature is 220k.
- Heat generation on electronic circuits is 2W per card.
- Model is constrained by stainless steel bars.

Material	E (Gpa)	k (W/m K)	CTE ( $\mu\text{m} / \text{m}^\circ\text{C}$ )
Copper	110	385	16.4
FR4 PCB	4.8	0.3	14
Silica Detector	112.4	124	2.3
304L	193	16.2	16.9

Table 6.3 characteristics of the materials



### Thermal-Mechanical Results

More information can be found in *Appendix D*.

The stainless steel bars will sustain most of the transversal deformation, but there is relevant deformation in ZZ (perpendicular to the detector); (*Figure 6.16 and 6.17*).

A total deformation of approximately **0.6mm** occurs due to slight “buckling” movement of the detector frame. It can also notice that the detector itself deforms less than 0.35mm.

By calculating the Von Misses stress, one can conclude that the detector is subjected to almost 50% less stress in comparison to the initial 4 edge model (*Figure 6.18*).

This factor must be taken into consideration, whichever model is built. Another simulation may be studied by attaching the detector on 2-3 key points and not one whole edge. And some other small changes can be done to improve the overall stress levels throughout the copper frame.

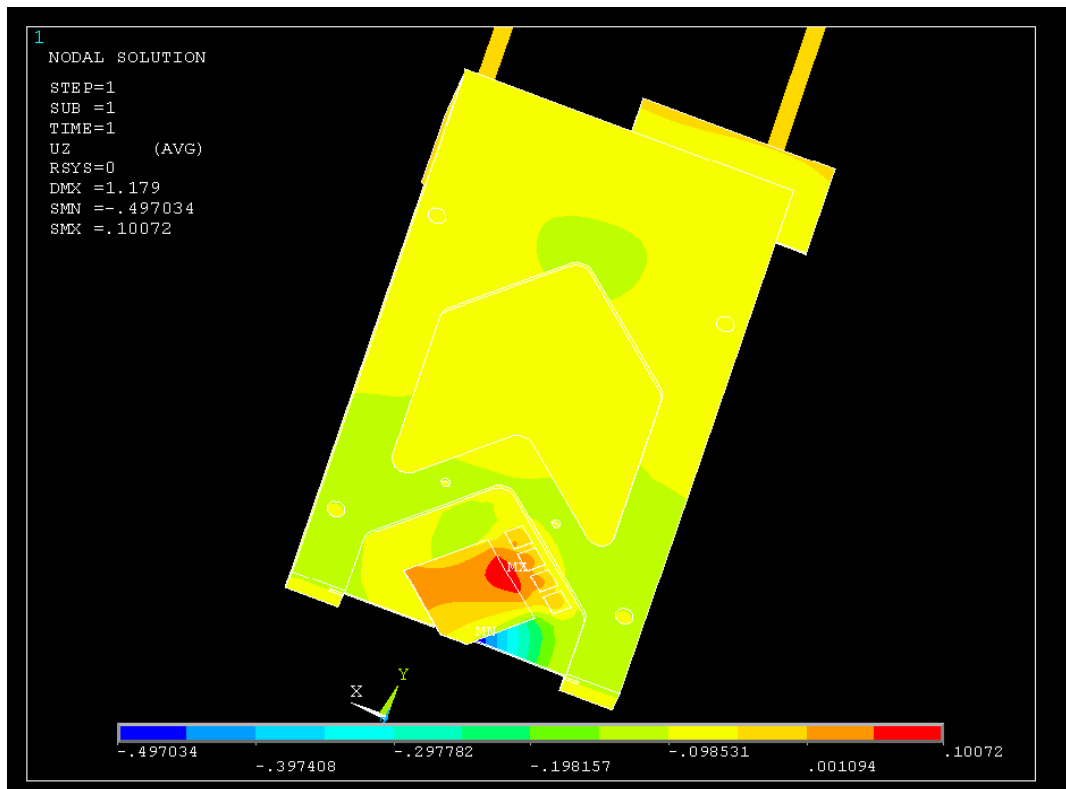


Fig 6.16 deformation in ZZ (perpendicular to the detector)



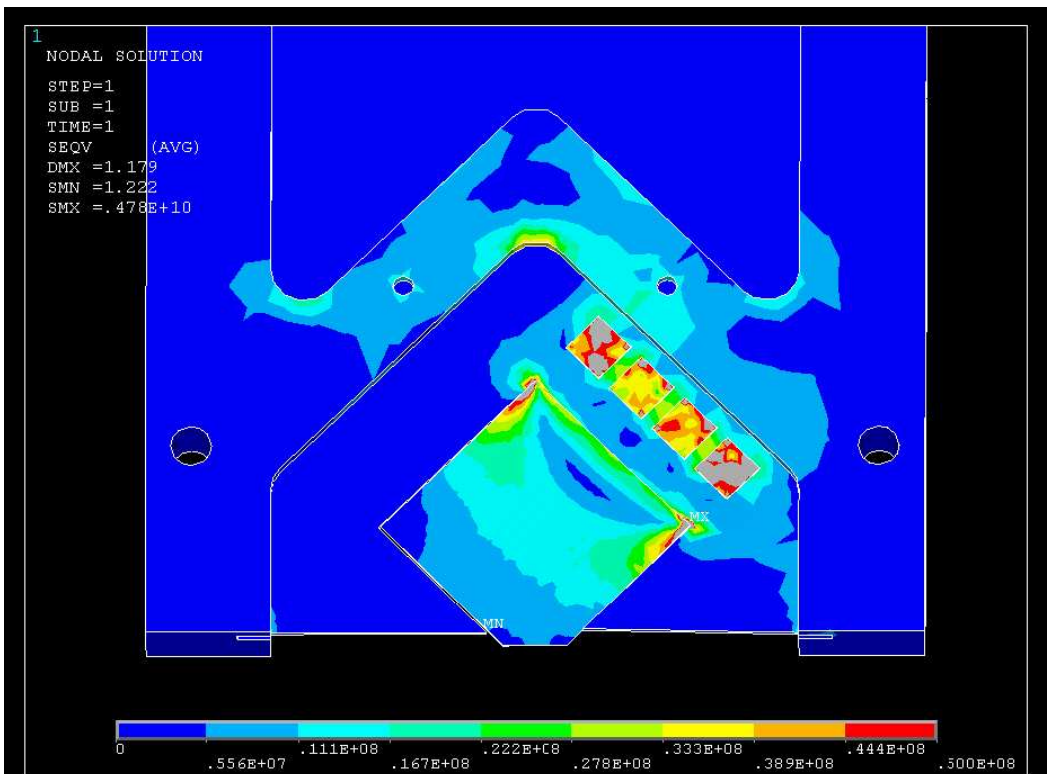
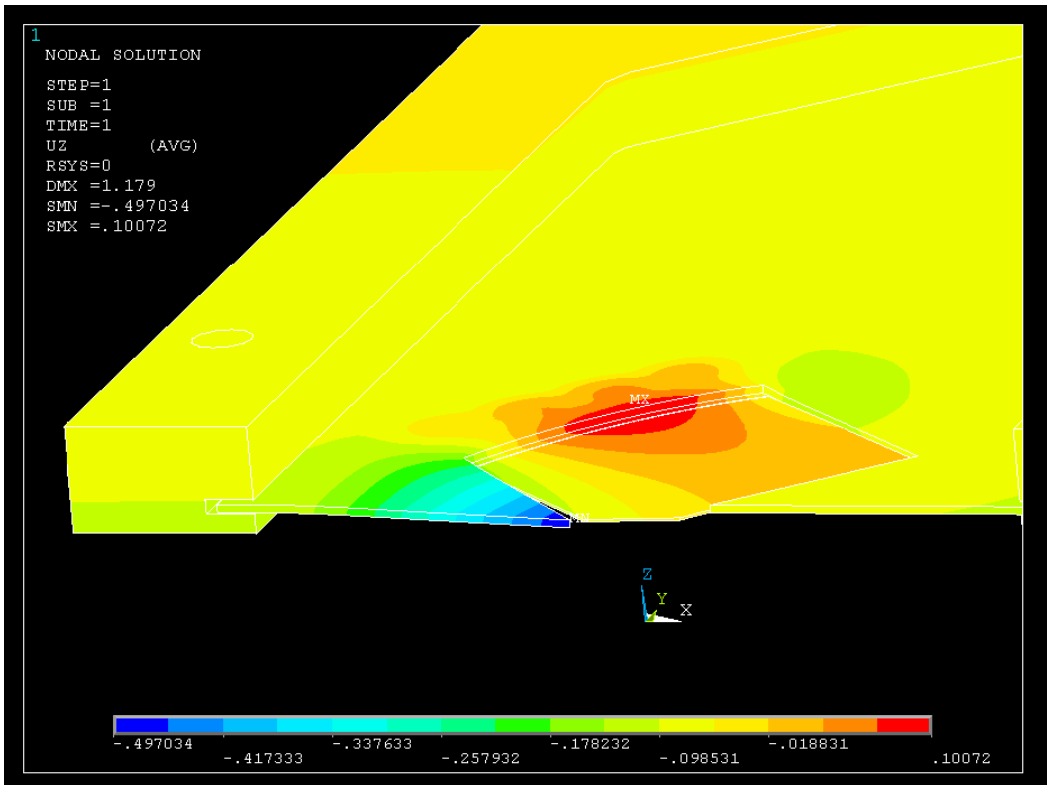


Fig 6.a.17 deformation in ZZ and Fig 6.a.18 Von Misses application



## Conclusions

These simulations have described some understanding on how each material reacts to the different variables imposed on the thermal model.

According to these pictures (*Figure 6.16 and 6.17*) can easily be verified that the detector can only be attached on one side to the PCB card.

An other conclusion it is that if there is a near perfect thermal / mechanical connection between cards the thermal model can satisfy our scientific needs. Therefore more study should be done in this aspect.

The results will be perfected once it be complete the transient analysis, and once it be simulated all 10 cards. At that moment it has thought about changing materials or the actual design of the thermal model whenever a critical point is detected.

After compiling the measurements from the laboratory and from the test simulation it will be able to fully understand the inner depths of how the thermal model behaves under the most severe conditions.



## 6.5 Assembly of the instruments on the Model

Once the sensors were correctly glued to the cards, it was necessary to prepare all the instrumentation wires.

First the wires were soldered to the sensors and filmed heaters (*Figure 6.19*). They were all individually labelled in order to be precisely indicated with the LabView software. Once they were passed through the 'feed through' each wire had to be soldered to a '107A052 - 40 channel terminal'.

Each channel was checked with a potentiometer and for the PT100 a nominal tension of 100volts must be reached to ensure a precise measurement. And 350ohms for the strain gauges.

All specifications are typical and have to be adjusted according to the cable construction and dimensions.

A similar procedure was done with the Strain Gauge instrumentation cables.

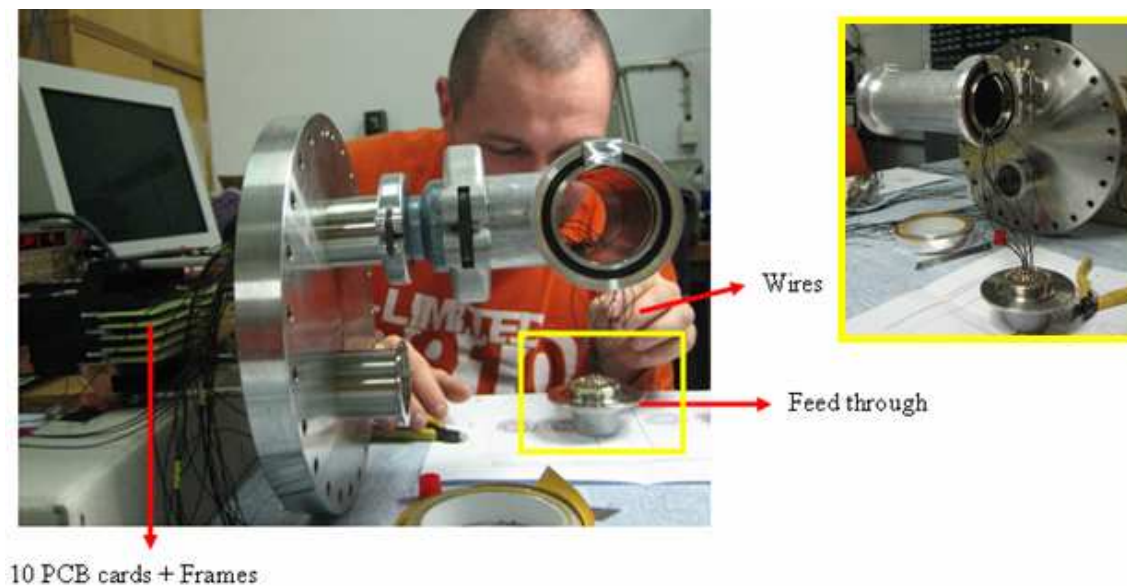


Fig 6.19 Assembly of the instrumentation on the model



An initial trial assembly was carried out in order to verify if all the components could easily be interconnected (*Figure 6.20*).

Some problems occurred, but were promptly corrected. One of the obstacles was to slide the heat pipes into the copper frame and fix them properly so that all there movement would be constrained.

Another problem was the very difficult access of the fixation screws and to pass the instrumentation wires.



Fig 6.20 Preliminary assembly of the instrumentation on the model



## 6.6 Preparing of a Data Acquisition in LabView

To interpret the measurements acquired by the PT100 and Strain Gauges sensors, a data acquisition software had to be compiled. (A complete overview of the LabView program structure can be found in the *Appendix E*.)

LabView® version 7.1 from National Instrumental was the software selected to be used [19]

Briefly, the LabView program serves to take all the measurements made by the sensors during the experiment, converting the tension output to the real variable that is being measured.

It was programmed with the objective to graphically represent arrays with all the data. The user is able to choose the time frame for each measurement and which channels to activate, in this case, which temperature sensors the user wants to use (*Figure 6.21 and 6.22*).

According to our necessities the interface can be changed.

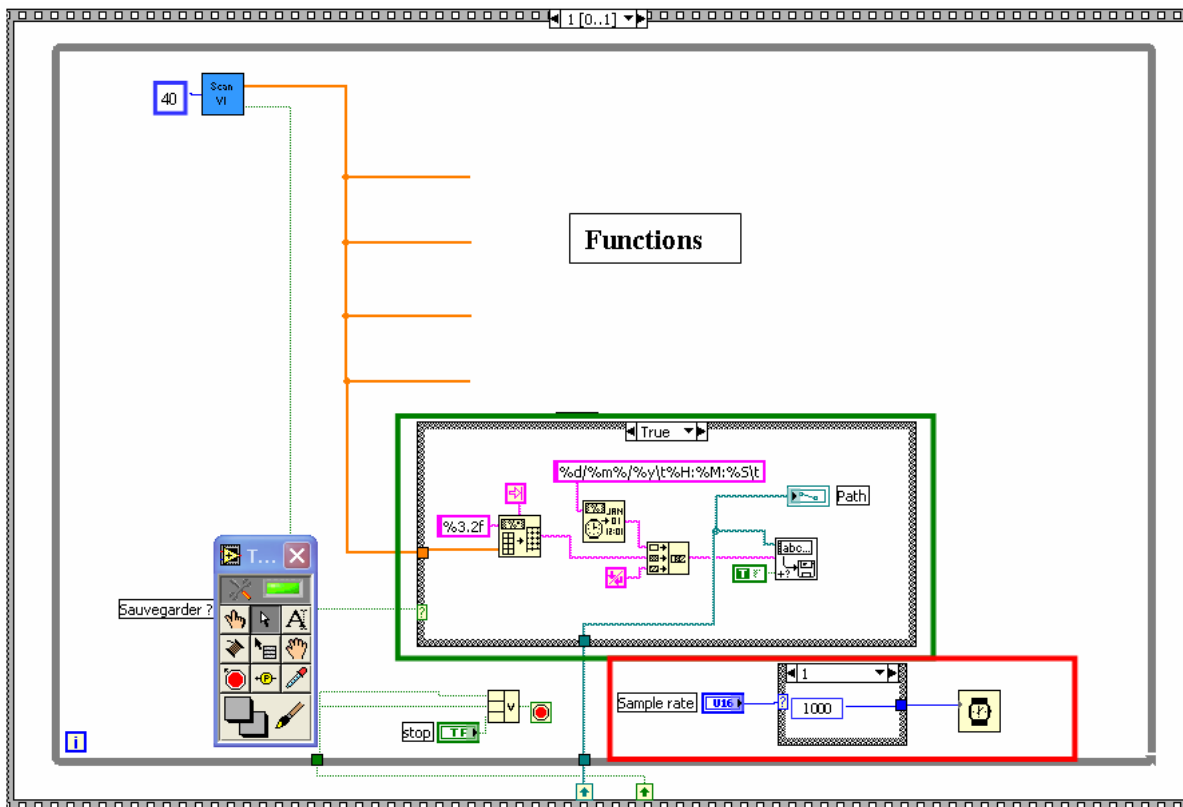


Fig 6.21 Interface of the algorithmic program “Block panel”



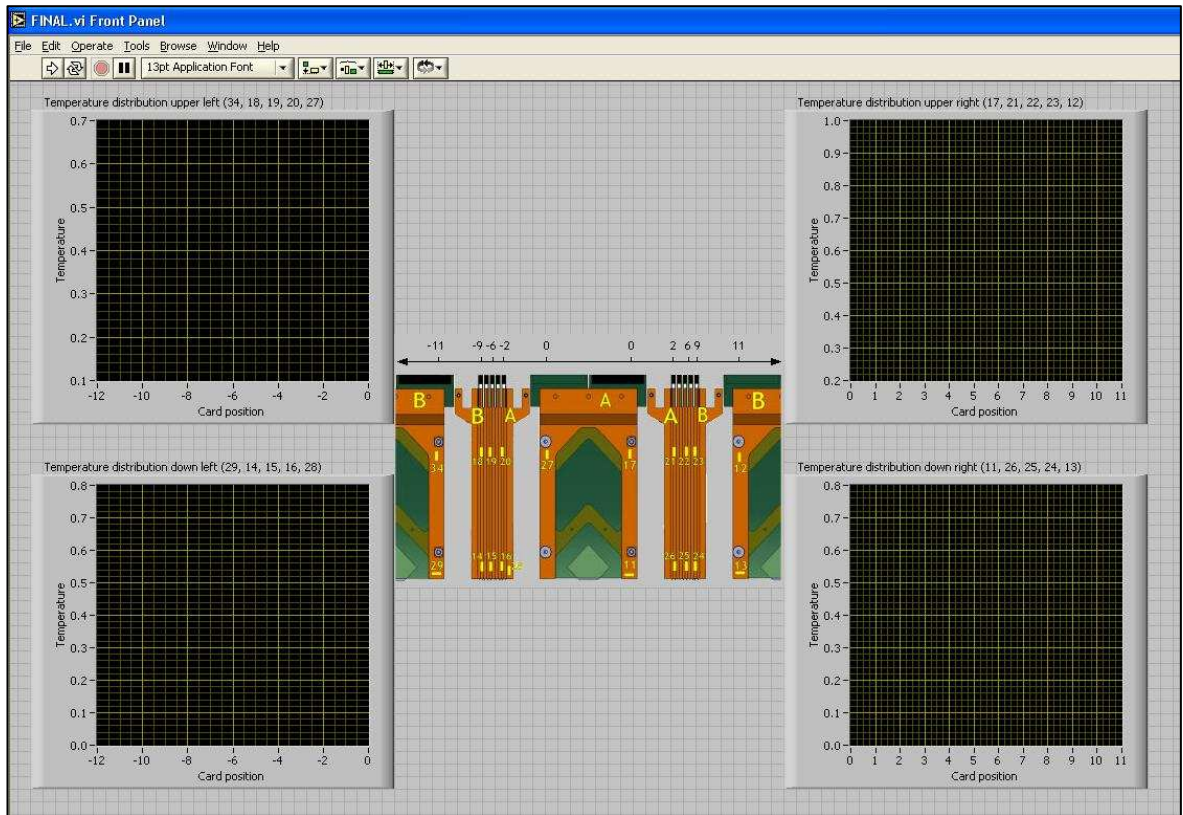


Fig 6.22 Interface of the “Front panel”



## 7 Test of the Model and Cooling System

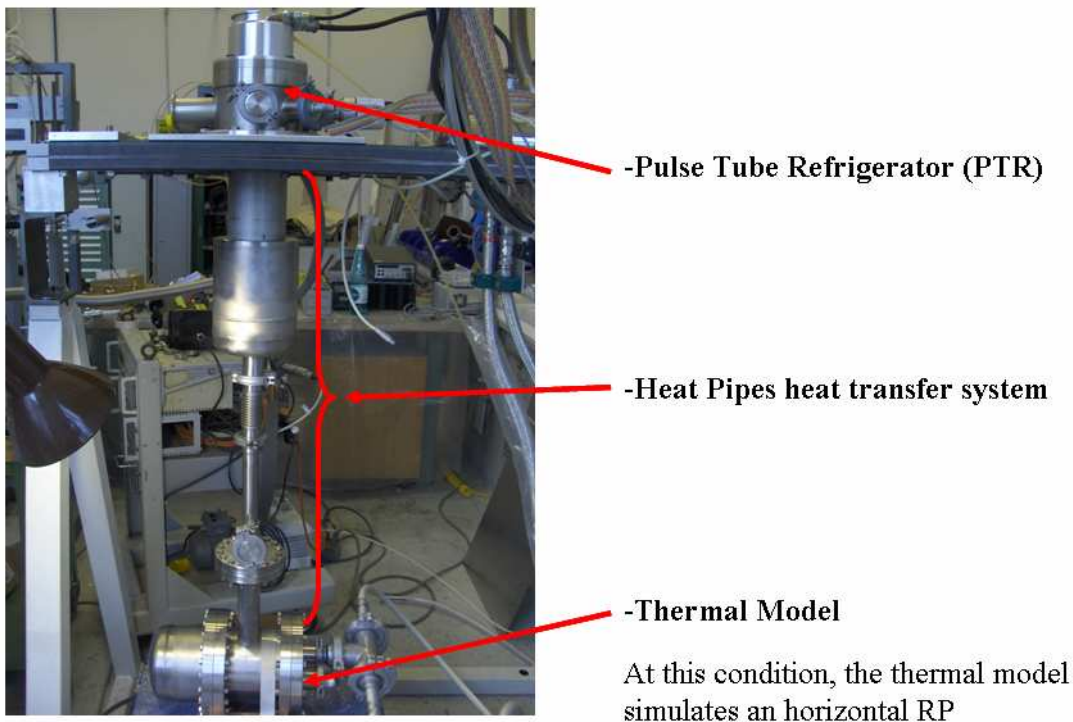
### 7.1 Data Analysis

#### 7.1.1 Thermal Test Station

A prototype was built and fully tested in the laboratory (*Figure 7.1*); in order to corroborate the precision of the results a FEM simulation was done. Some minor consideration must be taken into account:

- The model was cooled down to 210K.
- The heat generation (1W) was simulated by film heaters applied directly on the PCB FR4 card.
- There was a poor thermal contact between cards and the different materials.

#### Test Facility for a Roman Pot Thermal Model



The facility integrated in vacuum envelope

Fig 7.1 Roman Pot Thermal Model



### 7.1.2 Test Set-up for Roman Pot Thermal Model

#### 7.1.2.1 Temperatures on the copper frames-side

In order to know the temperatures on the frames side it was done a graphic about:

$$\text{Temperatures (K)} = f(\text{number of copper frame})$$

It was separated the results of the temperature sensors in two parts, the high part of the frame and the low part (nearest to the detector position).

Doing this experiment it was also realised the measurements with and without the heater.

For prudence it was applied on each heater 1W.

For understanding the results it was used the reference **¡Error! No se encuentra el origen de la referencia.**

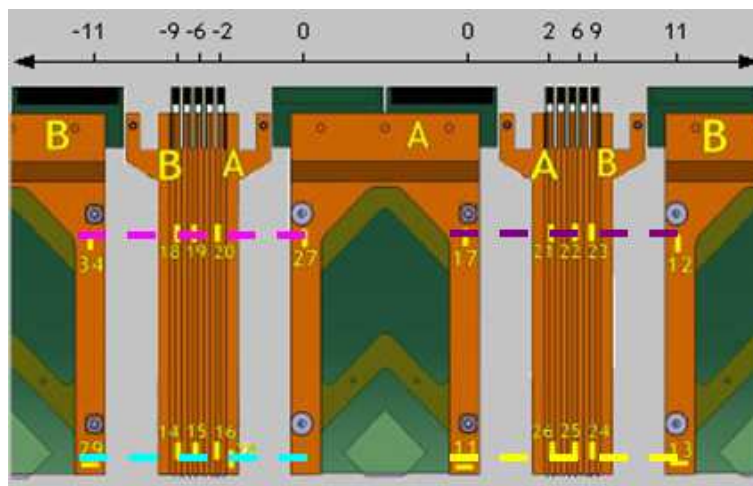


Fig 7.1 Temperature on the copper frame-side (Upper and Down)



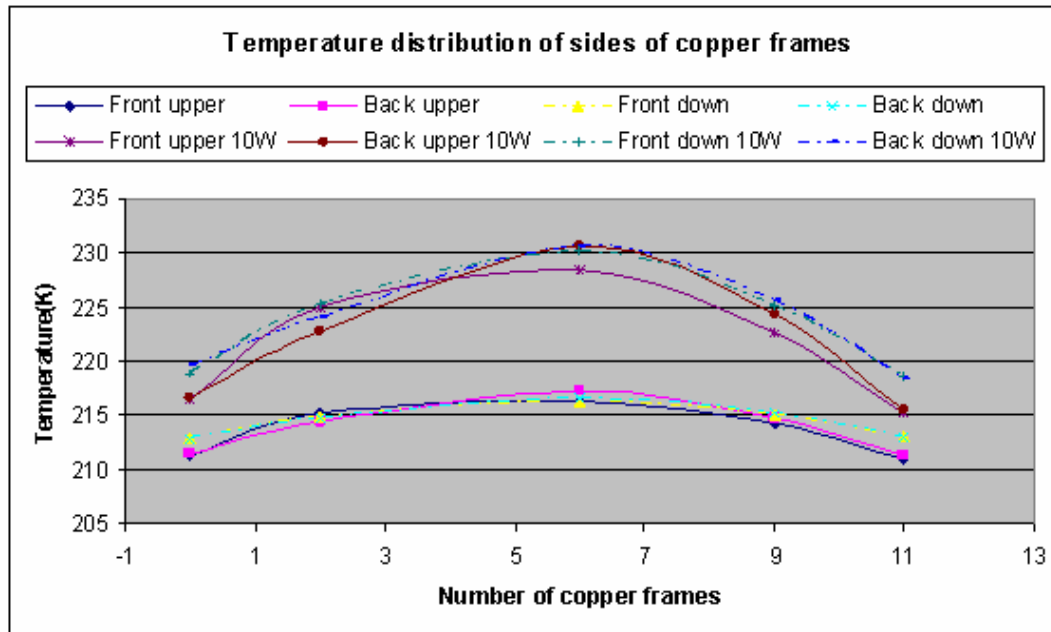


Fig 7.2 Temperature on the copper frame-side

Figure 7.2 shows the temperature distributions along the four cross-sections at the two sides of the copper frames. The conclusions of this Graphique are in the Table 7.1.

Parameter to measure	Heat load (W)	Variability of the temperature (K)
$\Delta T_{max}$	without	6.29
$\Delta T_{max}$	10	15.39

Table 7.1 Variability of the temperature on the upper/down frame



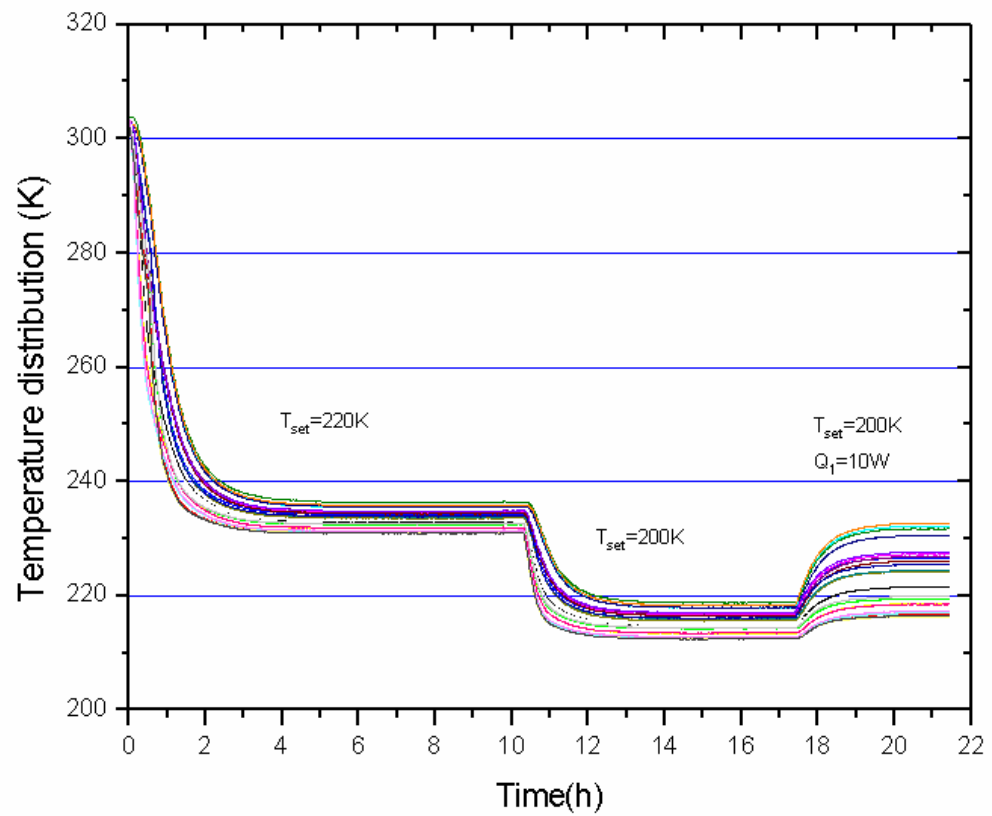


Fig 7.3 Temperature on the copper frame-side;  $[f(\text{time}(h))=\text{temperature}(k)]$

The reasons for the increase of the temperature can be for:

- Place of heat pipes
- Oxidized layer
- Without glue between copper frames



### 7.1.2.2 Temperatures on the copper frames-surfaces

It was placed 4 temperature sensors on the frame.

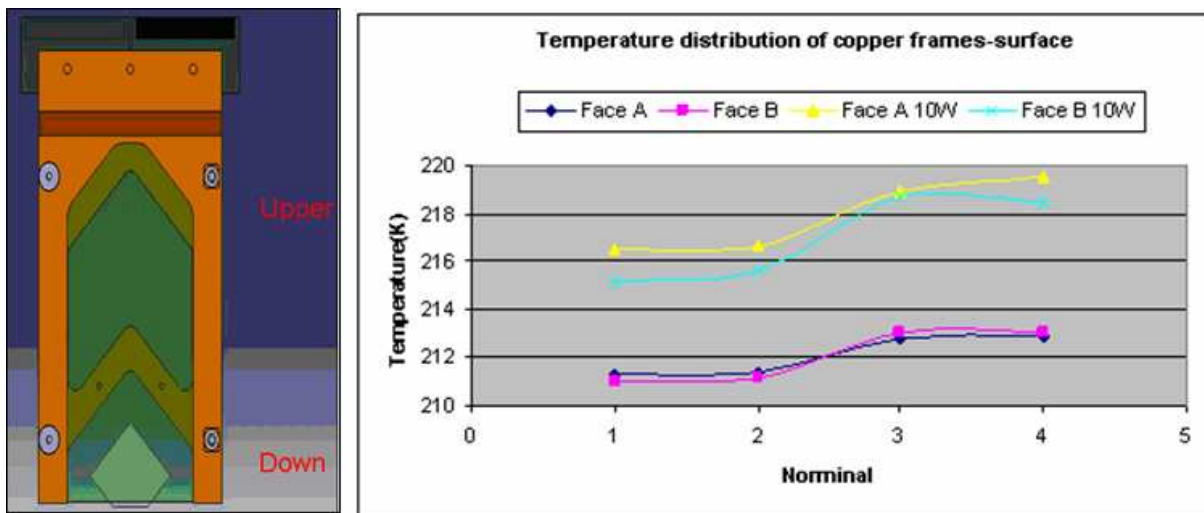


Fig 7.3 Temperature on the copper frame-surface

The main conclusions of the *Figure 7.3* are placed in the *Table 7.1*.

Parameter to measure	Heat load (W)	Variability of the temperature (K)
$\Delta T_{max}$	without	2.08
$\Delta T_{max}$ (down-upper)	10	3.21

Table 7.2 Variability of the temperature on the upper/down frame

The variability of the temperature on the copper frames-surfaces is almost stable. It can be concluded that the results follow the initial prediction.



7.1.2.3 Temperatures on the PCB cards

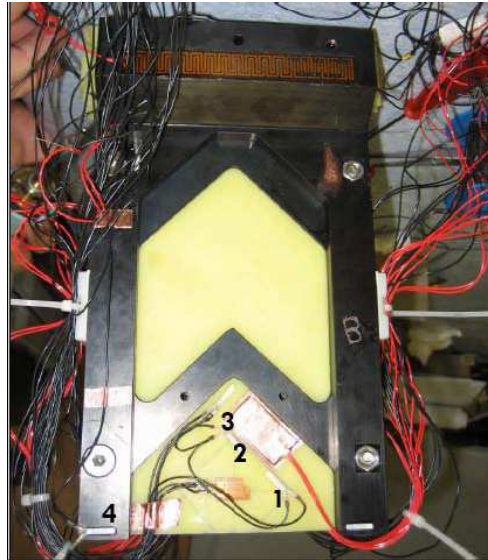


Fig 7.4 Temperatures on the first PCB card

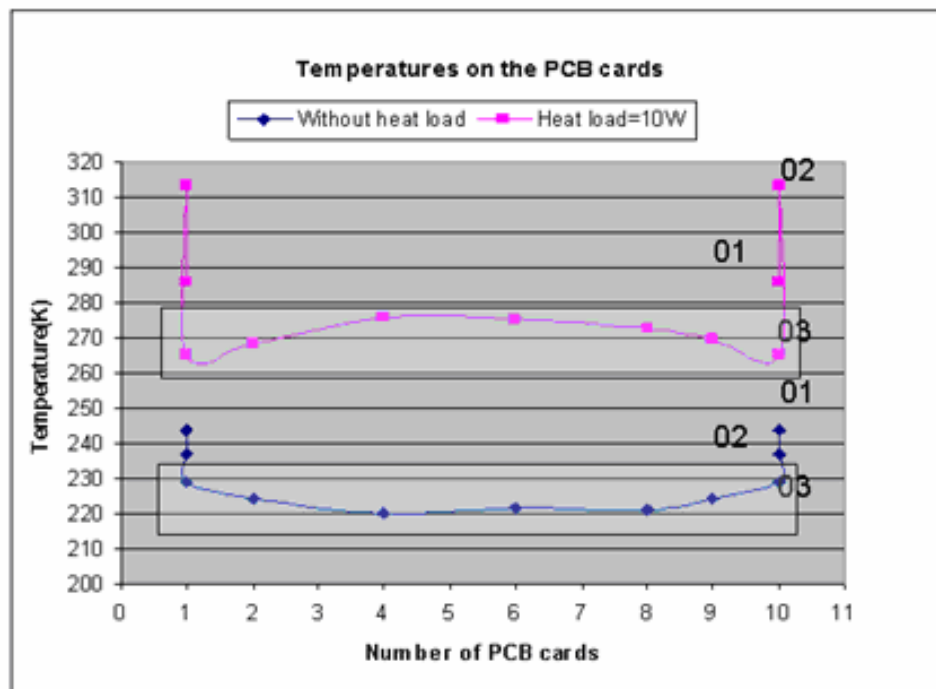


Fig 7.5 Temperatures on the PCB cards



The main conclusions of the *Figure 7.5* are placed in the *Table 7.3*.

**Temperature (K)**

Temperature Sensor	Measured	Simulated
1	290	[293 ; 309]
2	315	[309 ; 325]
<b>3</b>	<b>267</b>	[227 ; 244]
<b>4</b>	<b>220</b>	[211 ; 277]

Table 7.3 Temperatures on the first PCB card

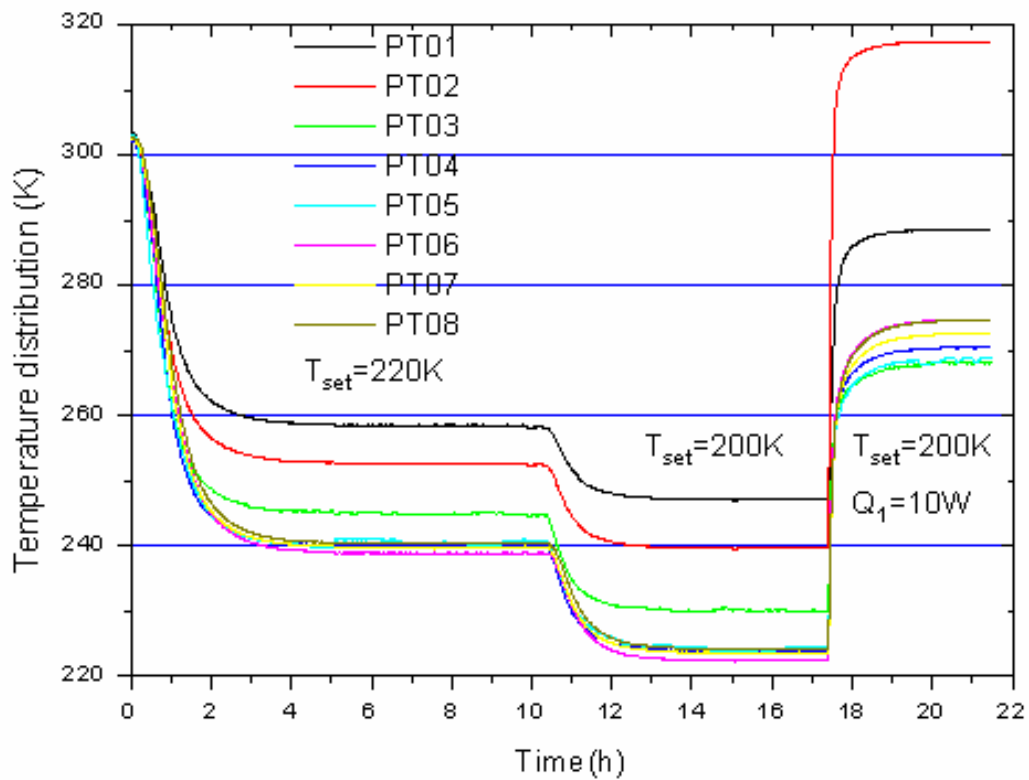


Fig 7.6 Temperatures on the PCB cards; [temperature(k) =f(time(h))]



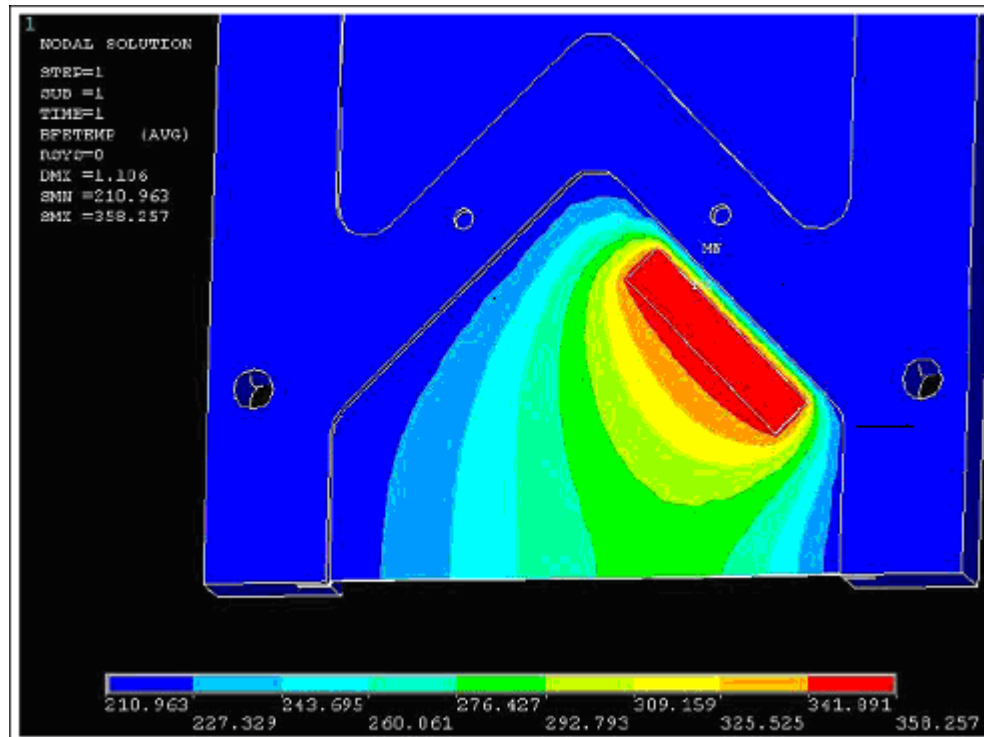


Fig 7.7 ANSYS; Temperatures on the PCB cards



## Edge Model

For this model the electronics and silica detector chip have been integrated. The detector has been attached to the PCB card on all 4 edges, and perfect thermal/mechanical contact has been assumed.

According to the Von-Misses calculation, the detector suffers 50 MPa stress on the contact edges. This is clearly a critical value; therefore a new simulation will be made, attaching the detector only on the edge.

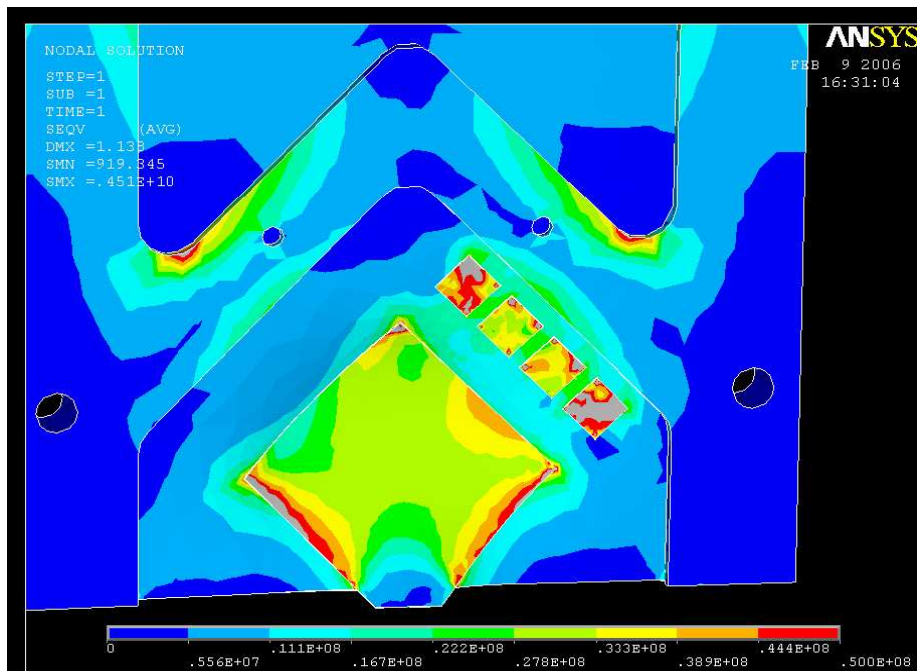


Fig 7.8 Temperatures on the PCB cards



### Unattached Model

In order to prevent any deformation of the silica detector and ensure that it would remain in its correct position throughout normal operation, it has been decided to attach the detector only on one edge.

### Temperature Distribution

The temperature Distribution shows a gradient of 7.6K.

The detector has a uniform temperature of 226K, due to the fact that it has only been attached to one edge of the PCB card.

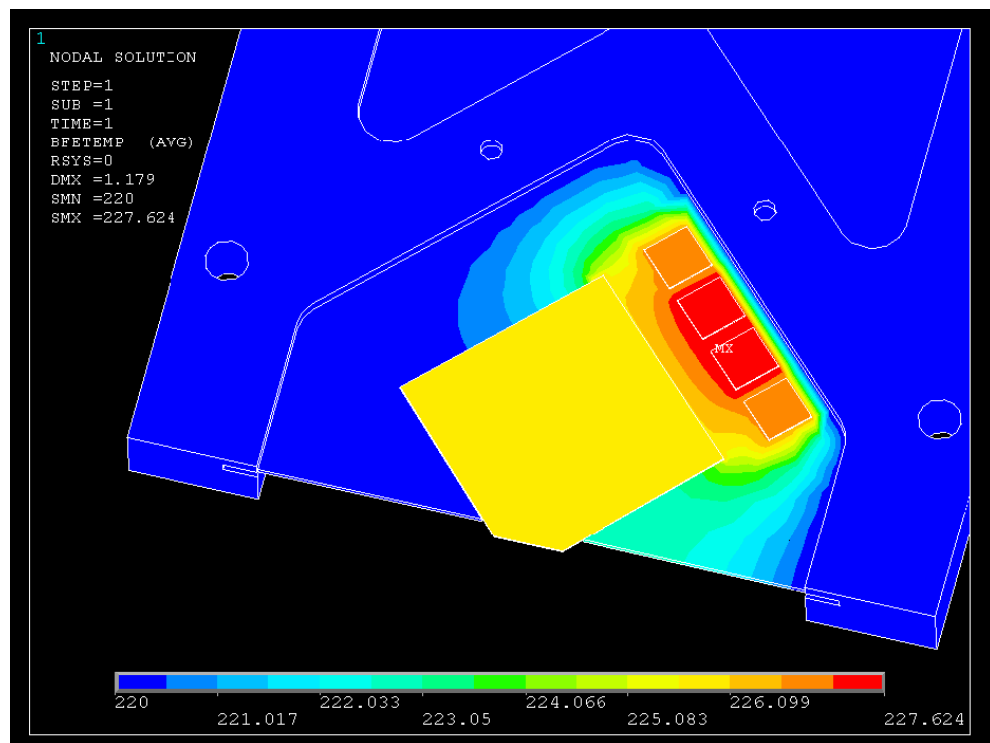


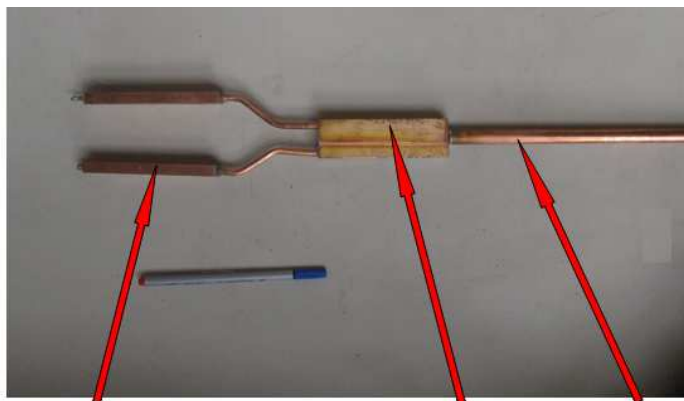
Fig 7.9 Temperatures on the PCB cards

Perfect contact between each material has been assumed, therefore the conduction will be steady and the heat dissipation will be maximum, i.e. the heat pipes will be able to continuously cool down the PCB card.



### 7.1.2.4 Temperatures on heat transfer system

Figure 7.10 shows all the parts of the cooling system



Two miniature Heat Pipes      Thermal Connector      "Big" Heat Pipe

Fig 7.10 Components of the cooling system

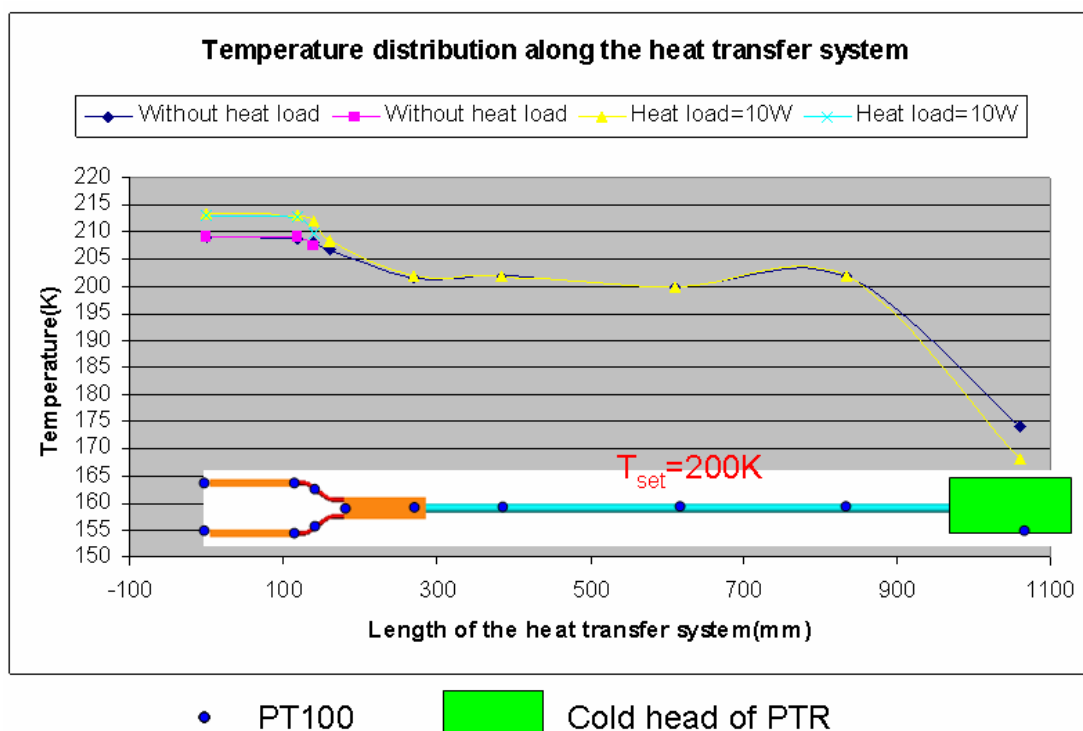


Fig 7.11 Temperatures distribution along the heat transfer system



After to analyse the Figure 7.11 it can be concluded that the big heat pipe works perfectly allowing us a broad range of working temperatures and a very versatile cooling system. It was found no difficulties when cooling down the copper frame to 210 K. Some problems can be considered when the big heat pipe is nearest to the pulse tube.

## 7.2 Conclusion

- Heat pipes and the heat transfer system perform well.
- All temperatures are constant after the system is under stable condition.
- Temperature distribution on copper frame almost uniform.
- Large temperature gradients among different positions on the PCB card ( $\Delta T_{\max}=19.6\text{K}$  without heat load;  $\Delta T_{\max}=49.4\text{K}$  10W).
- Large temperature gradients between PCB card and copper frame at the condition of heat load input ( $\Delta T_{\max}=100\text{K}$  10W).

In this experiment it can be concluded that the heat pipes work perfectly allowing us a broad range of working temperatures and a very versatile cooling system. And we found no difficulties when cooling down the copper frame to 210 K.

On the other hand, it can be easily see that the PCB has very poor thermal properties and over heat when 1 watt was generated by the film heaters. Therefore it must choose different materials and improve the gluing of each card.





## 8 Future developments

As of this May 2006, the project of “Thermal Model” has been put on hold because another group of TOTEM is developing an alternative cooling system. When the other group’s research is complete, the TOTEM collaboration will choose which one is the best for the TOTEM experiment.

Should the project “Thermal Model” be chosen, future work will require the modification of some pieces; new materials are needed in order to improve the conductivity on the cards. Also, it is essential to change the copper material for the structure because it is very heavy and makes transportation and work difficult.

Some ideas for the development of a new cooling system include using a Loop Heat Pipe or to locate one small pulse tube on each Thermal Model.

The deadline for the TOTEM project completion is next October. Every thing has to be ready at that time for installation at the Point 5, where the TOTEM experiment will be located.



## 9 Conclusions

This project describes the procedure used to successfully create the Thermal Model and to implement the cooling system proposed by the TOTEM collaboration in order to obtain satisfactory results.

- After performing all tests of the heat pipes, where working parameters were changed, such as, dimensions of the heat pipes, kind of heat pipes, working fluid, power applied, wick structure, disposition of the test (gravity assisted, horizontal or anti-gravity), it was concluded that for the Thermal Model experiment the kind of heat pipes that could be used are:
  - Small Mesh Heat pipe [L= 300mm; Ø= 6mm] fills with 3.5g of Xenon
  - Big Groove Heat Pipe [L=950mm; Ø= 12.7mm] fills with 5g of propane
- After trying different position of the heat pipe, one can extract the following conclusions:
  - Gravity assisted the most efficient
  - Antigravity the worst
  - Gravity helps for 40% of the heat transfer
- To perform the evaluation of the thermo-dynamical behaviour, 40 temperature sensors were installed along several key points of the prototype (either on the copper frame or the PCB cards).
- Simulations have allowed for an understanding about how each material reacts to the different variables imposed on the Thermal Model.
- According to the ANSYS pictures about the deformation ZZ on the Strain Gauges, it can easily be verified that the detector can only be attached on one side of the PCB card.
- An other conclusion is that if there is a near perfect thermal / mechanical connection between cards, the Thermal Model can satisfy our scientific needs. Therefore, more study should be done in this aspect.
- The results will be perfected once it be completed the transient analysis, and once all 10 cards can be simulated. At that it be can considered changing materials or the actual design of the Thermal Model whenever a critical point is detected.
- After compiling the measurements from the laboratory and results from the test simulation it will be able to fully understand the inner depths of how the Thermal



Model behaves under the most severe conditions.

- Heat pipes and the heat transfer system perform well.
- All temperatures are constant after the system is under stable operating conditions.
- The temperature distribution on the copper frame is almost uniform.
- Large temperature gradients exist among different positions on the PCB card ( $\Delta T_{\max}=19.6\text{K}$  without heat load;  $\Delta T_{\max}=49.4\text{K}$  10W).
- Large temperature gradients exist between the PCB card and copper frame which depend on the condition of the heat-load input ( $\Delta T_{\max}=100\text{K}$  10W).
- It can be concluded that the heat pipes work perfectly allowing us a broad range of working temperatures and a very versatile cooling system. It was found no difficulties when cooling down the copper frame to 210 K.
- On the other hand, it can be easily seen that the PCB has very poor thermal properties and overheats when 1 Watt is generated by the film heaters. Therefore, different materials should be chosen and the gluing of each card improved.





## 10 Acknowledgements

I would like to thank Dr. Francisco Calviño of ETSEIB for his supervision on this project and for his kind support over this whole period here at CERN.

I have to express my sincere thanks to Dr. Friedrich Haug, my supervisor at CERN, for giving me the chance to develop this project. His leadership, amabiliity and experience have provided me with a lot of confidence and have been very useful during my work time.

Thanks to Sylvain Rvat for helping me with the LabVIEW program, for his spent time in resolving my doubts, for his documentation... because his aid was really useful.

For being my office-mates and friends, because they have made my integration at CERN easier and for great conversations we had, I would like to specially thank Jihao Wu, Jeremy Moulyere, Phillip Santos, Fabian Roesler and Hugo Pinto Pereira. It has been a pleasure to work with all the members of the AT/ECR section. The working atmosphere has been excellent.

Special thanks to Dr. Antonio Vergara, Esther Barbero, Oscar Fernandez, Andres Gomez, Alex Barriuso, Raquel Fandos, Monica Moles, Ivan Podadera who always found time to correct most aspects of my thesis.

And, of course, thanks to all my friends in Geneve, who made these 14 months in Geneva one of the best periods on my life, which I will never forget. Thanks a lot.

Gracies als meus pares, Rosa Maria i Joan, per tot el que han fet, el que fan i el que seguiran fent per mi. Us estimo!. A ma germana, Núria i al meu cunyat Enrique per donar-me apoio cada cop que le necessitat; al meu germà, Roger i la Montse. Als meus avis, tiets i cosins per cuidar-me amb tant de carinyo.

Gracies a la Cristina V, la Izaskun, la Tània, la Cristina B, la Marta M, l'Helena, la Marta B i la Mònica per cuidar Reus quant jo no hi era. Us he trobat a faltar. Als meus companys de la univiersitat, com oblidar els sopars, els fetes, les hores a la biblioteca, els mals de panxa de la carrera i l'amistad. A les meves companyes de pis, Eva i Tània, per les moltes hores que hem passat juntes, per les comprenssions i la vostra amistad.

And I don't want to finish without thanking Dave for his loving support and patience throughout all this period.





## 11 References

- [1] <http://public.web.cern.ch/public/about/aboutCERN.html>
- [2] The LHC Study Group. LHC the Large Hadron Collider – Conceptual Design Vol. II. CERN/AC/95-05, October 1995. <http://lhc.web.cern.ch/lhc/general/general.htm>
- [3] R. Schmidt. Accelerator Physics and Technology of the LHC. CERN Yellow Report 99-01, 1998.
- [4] TOTEM LOI, Letter of intend, CERN/LHCC 97-49,1997
- [5] <http://totem.web.cern.ch/Totem/>
- [6] TOTEM, Technical Design Report, CERN-LHCC-2004-002, 7.1.2004
- [7] Haruyama, T., et all., Development of a high-poer coaxial pulse tube refrigerator for a liquide xenon calorimeter, Proceedings of the CEC, Anchorage, 2003 (to be published).
- [8] Dunn, P.D. and D.A Reay, Heat Pipes, Fourth Edition, Pergamon Press, 1994.
- [9] Amir Faghri Taylor & Francis Publisher, Heat Pipe Science and Technology, 1995
- [10] Robert DeHo\_ and Kevin Grubb, Heat pipe application guidelines, Thermacore Inc.
- [11] Shandor Dektor, Heat pipes at TOTEM, CERN
- [12] Shankara Narayanan K.R., What is a heat pipe, <http://www.cheresources.com>, 2004
- [13] E.G. Alexander, Structure-property relationships in heat pipe wicking materials, Ph.D. Thesis, Department of Chemical Engineering, North Carolina State University, Raleigh, NC, 1972
- [14] Gedeon D. Pulse tube model-class reference guide. Gedeson Associates; 1999
- [15] M.E. Will,A.T.A.M. de Waele, Ideal pulse-tube refrigerators with real gases, Journal of Applied Physics 98 (2005) 0449111-0449114
- [16] Strain Gauges; [http://www.allaboutcircuits.com/vol\\_1/chpt\\_9/7.html](http://www.allaboutcircuits.com/vol_1/chpt_9/7.html); February 2006
- [17] Measuring the Strain Gauges;  
<http://zone.ni.com/devzone/conceptd.nsf/webmain/C83E9B93DE714DB08625686600704DB1> March 2006
- [18] ANSYS, User manual



[19] LabVIEW, User manual; April 2003 edition; 320999E-01

[20] Frank P. Incropera and David P. DeWitt. Fundamentos de transferencia de calor. Cuarta edición

### Other reference sources:

Other references sources have been used to complete all the information.

Cooling system:

- **Heat Pipe.** Google 02/24/05:

[http://www.electronics-cooling.com/Resources/EC\\_Articles/SEP96/sep96\\_02.htm](http://www.electronics-cooling.com/Resources/EC_Articles/SEP96/sep96_02.htm)

- **Heat Pipe.** Google 02/25/2005

<http://www.heatpipe.com/heatpipes.htm>

- **Heat sink testing links**

<http://www.overclockers.com/tips240/>

[http://www.burning-issues.co.uk/how\\_to/TakingaTemp/takingatemp01b.htm](http://www.burning-issues.co.uk/how_to/TakingaTemp/takingatemp01b.htm)

<http://www.burning-issues.co.uk/hardware/hotair/hotair.htm>

<http://www.burning-issues.co.uk/hardware/calibrating/calibrating.htm>

[http://www.coolingzone.com/Guest/News/NL\\_DEC\\_2000/Tony/TK\\_Dec\\_2000.html](http://www.coolingzone.com/Guest/News/NL_DEC_2000/Tony/TK_Dec_2000.html)

<http://www.anandtech.com/showdoc.html?i=1136>

- **Ingenieria Termica**

<http://personales.ya.com/universal/TermoWeb/IngenieriaTermica/Teoria/>

- **Física: Capilaridad y Termodinámica:**

<http://www.sc.ehu.es/sbweb/fisica/estadistica/otros/latente/latente.htm>

[http://www.levieuxcoq.org/Otro\\_Dico.html](http://www.levieuxcoq.org/Otro_Dico.html)

<http://personal.redestb.es/jesusrom/pompas/pompas0.html>

- **Heat Pipes:**

[http://www.electronics-cooling.com/Resources/EC\\_Articles/SEP96/sep96\\_02.htm](http://www.electronics-cooling.com/Resources/EC_Articles/SEP96/sep96_02.htm)

<http://www.sti.nasa.gov/tto/spinoff1996/64.html>

<http://www.heatpipe.com/heatpipes.htm>

<http://www.knap.at/de/noren.htm>



<http://www.waermeleitrohre.de/eng/wirk.htm>

<http://www.essentec.de/projekte.htm>

- **Heat Pipe, Google:** 02/28/2005

<http://www.tropic-kool.com/heatpipes.htm#benefits>

- **Variable conductance Heat Pipes:** 03/02/2005

<http://www.ichmt.org/abstracts/PTC-03/04-02.pdf>

- **Heat Pipe:** 03/02/2005

<http://ej.iop.org/links/q95/AytWQ6RB1gifU8TGeIg97A/ptv16i2p69.pdf>

- **Heat Pipe, Wick structure:** 04/03/2005

[http://www.electronics-cooling.com/html/2004\\_nov\\_a1.html](http://www.electronics-cooling.com/html/2004_nov_a1.html)

- **Electronic Heat Pipe:** 04/03/2005

<http://www.nasatech.com/Briefs/July98/0798ETB1.html>

- **Dibujo animado de una heat pipe:** 05/03/2005

<http://www.heatpipe.co.kr/product3.html>

- **Friedrich info:** 10/03/2005

<http://www.thermacore-europe.com/scripts/salesreps/switzliech.html>

